Numerical simulation of a Cascadia Subduction Zone (CSZ) type tsunami with application to Boundary Bay in the Southern Strait of Georgia under future global sea level conditions

Isaac V. Fine and Richard E. Thomson

Fisheries and Oceans Canada
Institute of Ocean Sciences
9860 West Saanich Road
Sidney, BC V8L 4B2

2026

Canadian Technical Report of
Hydrography and Ocean Sciences 416

Fisheries and Oceans Canada | Pêches et Océans Canada

Canada

Canadian Technical Report of Hydrography and Ocean Sciences

Technical reports contain scientific and technical information of a type that represents a contribution to existing knowledge, but which is not normally found in the primary literature. The subject matter is generally related to programs and interests of the Oceans and Science sectors of Fisheries and Oceans Canada.

Technical reports may be cited as full publications. The correct citation appears above the abstract of each report. Each report is abstracted in the data base Aquatic Sciences and Fisheries Abstracts.

Technical reports are produced regionally but are numbered nationally. Requests for individual reports will be filled by the issuing establishment listed on the front cover and title page. Regional and headquarters establishments of Ocean Science and Surveys ceased publication of their various report series as of December 1981. A complete listing of these publications and the last number issued under each title are published in the Canadian Journal of Fisheries and Aquatic Sciences, Volume 38: Index to Publications 1981. The current series began with Report Number 1 in January 1982.

Rapport technique canadien sur l'hydrographie et les sciences océaniques

Les rapports techniques contiennent des renseignements scientifiques et techniques qui constituent une contribution aux connaissances actuelles mais que l'on ne trouve pas normalement dans les revues scientifiques. Le sujet est généralement rattaché aux programmes et intérêts des secteurs des Océans et des Sciences de Pêches et Océans Canada.

Les rapports techniques peuvent être cités comme des publications à part entière. Le titre exact figure au-dessus du résumé de chaque rapport. Les rapports techniques sont résumés dans la base de données Résumés des sciences aquatiques et halieutiques.

Les rapports techniques sont produits à l'échelon régional, mais numérotés à l'échelon national. Les demandes de rapports seront satisfaites par l'établissement auteur dont le nom figure sur la couverture et la page de titre.

Les établissements de l’ancien secteur des Sciences et Levés océaniques dans les régions et à l'administration centrale ont cessé de publier leurs diverses séries de rapports en décembre 1981. Vous trouverez dans l'index des publications du volume 38 du Journal canadien des sciences halieutiques et aquatiques, la liste de ces publications ainsi que le dernier numéro paru dans chaque catégorie. La nouvelle série a commencé avec la publication du rapport numéro 1 en janvier 1982.

Canadian Technical Report of
Hydrography and Ocean Sciences 416

2026

NUMERICAL SIMULATION OF A CASCADIA SUBDUCTION ZONE (CSZ) TYPE TSUNAMI WITH APPLICATION TO BOUNDARY BAY IN THE SOUTHERN STRAIT OF GEORGIA UNDER FUTURE GLOBAL SEA LEVEL CONDITIONS

By

Isaac V. Fine and Richard E. Thomson

Fisheries and Oceans Canada
Institute of Ocean Sciences
9860 West Saanich Road
Sidney, BC V8L 4B2

Cat. No. Fs 97-18/416E-PDF ISBN 978-0-660-99248-8 ISSN 1488-5417

Correct citation for this publication:

Fine, I.V., and Thomson, R.E. 2026. Numerical simulation of a Cascadia Subduction Zone (CSZ) type tsunami with application to Boundary Bay in the Southern Strait of Georgia under future global sea level conditions. Can. Tech. Rep. Hydrogr. Ocean Sci. 416: v + 60 p.

CONTENTS

1. INTRODUCTION……..1

2. MODEL SETUP…….2

2.1. Nested Grid Formulation……...2

2.2. Sea Level Rise Scenarios……..…….…8

2.3. Dike Height at Boundary Bay Shore…….12

2.4. Model Reference Level……19

2.5. The Source Distribution……..……...20

3. RESULTS……..…22

3.1. Maximum Tsunami Wave Heights for the Coarse and Intermediate Grids…….…22

3.2. Detailed Results for Boundary Bay: Variations of Sea Levels and Tsunami-Induced Currents……..…..….28

4. CONCLUSIONS……..…..57

ACKNOWLEDGEMENTS…….……58

REFERENCES…….……..……..59

ABSTRACT

Fine, I.V., and Thomson, R.E. 2026. Numerical simulation of a Cascadia Subduction Zone (CSZ) type tsunami with application to Boundary Bay in the Southern Strait of Georgia under future global sea level conditions. Can. Tech. Rep. Hydrogr. Ocean Sci. 416: v + 60 p.

Estimation of the tsunami risk to the British Columbia coast from events similar to the 1700 Cascadia Subduction Zone (CSZ) M_w 9.0 earthquake is of considerable importance to low-lying areas of British Columbia such as Boundary Bay. This risk is expected to increase as global sea level continues to rise due to global warming. A state-of-the-art numerical model, based on newly available high-resolution bathymetric and topographic data, was used to estimate the impact of a CSZ tsunami on Boundary Bay under three future sea level rise scenarios: Scenario-1 (S1) a 0.5 m global sea level rise; Scenario-2 (S2), a 1 m global sea level rise; and Scenario-3 (S3), a 2 m global sea level rise. Each scenario takes into account local tectonic movement and changes in ocean circulation. The main findings are: (1) scenarios S2 and S3 show the need for an increase in dike heights along parts of Boundary Bay and the Serpentine and Nicomekl rivers. Without these changes, flooding would occur before any tsunami waves arrive in the area; (2) the Boundary Bay tsunami will reach 1.6 m above the local tidal level for all three scenarios. The first wave will be the highest; (3) tsunami wave amplitudes in Boundary Bay will be non-uniform, with the highest waves impacting Mud Bay and Drayton Harbor; (4) scenario S3 tsunami waves will overflow the updated dike at Mud Bay and Boundary Bay Park; and (5) the tsunami will induce strong currents at the entrance to Drayton Harbor (up to 4 m/s), at the mouth of the Nicomekl River (up to 3 m/s), and at the mouth of the Campbell River (up to 2 m/s). As sea level rises, the current speed increases in the entrances to the rivers, but decreases at the entrance to Drayton Harbor.

RÉSUMÉ

Fine, I.V., and Thomson, R.E. 2026. Numerical simulation of a Cascadia Subduction Zone (CSZ) type tsunami with application to Boundary Bay in the Southern Strait of Georgia under future global sea level conditions. Can. Tech. Rep. Hydrogr. Ocean Sci. 416: v + 60 p.

L'estimation du risque de tsunami sur la côte de la Colombie-Britannique, découlant d'événements similaires au séisme de magnitude 9,0 survenu dans la zone de subduction de Cascadia (ZSC) en 1700, revêt une importance considérable pour les zones basses de la Colombie-Britannique, comme Boundary Bay. Ce risque devrait augmenter à mesure que le niveau mondial de la mer continue d'augmenter en raison du réchauffement climatique. Un modèle numérique de pointe, basé sur des données bathymétriques et topographiques à haute résolution récemment disponibles, a été utilisé pour estimer l'impact d'un tsunami dans la ZSC sur Boundary Bay selon trois scénarios d'élévation future du niveau de la mer: Scénario 1 (S1): une élévation globale du niveau de la mer de 0,5 m; Scénario 2 (S2): une élévation globale du niveau de la mer de 1 m; et Scénario 3 (S3): une élévation globale du niveau de la mer de 2 m. Chaque scénario prend en compte les mouvements tectoniques locaux et les changements dans la circulation océanique. Les principales conclusions sont les suivantes: (1) les scénarios S2 et S3 montrent la nécessité d'augmenter la hauteur des digues le long de certaines parties de Boundary Bay et des rivières Serpentine et Nicomekl. Sans ces changements, les inondations se produiraient avant que les vagues du tsunami n'atteignent la zone; (2) le tsunami de Boundary Bay atteindra 1,6 m au-dessus du niveau de marée local pour les trois scénarios. La première vague sera la plus haute; (3) les amplitudes des vagues du tsunami à Boundary Bay ne seront pas uniformes, les vagues les plus hautes impactant Mud Bay et Drayton Harbor; (4) les vagues du tsunami du scénario S3 déborderont la digue modernisée à Mud Bay et au parc de Boundary Bay; et (5) le tsunami induira de forts courants à l'entrée de Drayton Harbor (jusqu'à 4 m/s), à l'embouchure de la rivière Nicomekl (jusqu'à 3 m/s) et à l'embouchure de la rivière Campbell (jusqu'à 2 m/s). À mesure que le niveau de la mer monte, la vitesse du courant augmente aux entrées des rivières, mais diminue à l'entrée de Drayton Harbor.

1. INTRODUCTION

Cascadia Subduction Zone (CSZ) tsunamis are the main tsunami threat for the west coast of British Columbia (Clague et al., 2003; Leonard et al., 2014). The Great CSZ earthquake of 26 January 1700 (moment magnitude, M_w 9.0) generated a major trans-oceanic tsunami that caused significant destruction in Japan and strongly affected the west coasts of the USA and Canada. Results from recent paleotsunami studies along the coast of Vancouver Island and the west coast of the USA (cf. Clague, 2000), and preliminary numerical modelling of CSZ tsunamis for coastal North America (cf. Cherniawsky et al., 2007; Fine et al., 2008; Cheung et al., 2011, AECOM, 2013), demonstrate the high risk of CSZ tsunamis for British Columbia. Numerous seismotectonic studies indicate that great megathrust earthquakes in the CSZ region have occurred on a regular basis in the past and can be expected to occur with an average return period of about 500 years in the foreseeable future (Witter et al., 2013; Wang and Tréhu, 2016).

The 1100 km long CSZ extends from Cape Mendocino in northern California to central Vancouver Island (Figure 1). Subduction of the Pacific Plate beneath the North American Plate takes

place about 100 km to the west of Vancouver Island. Given the relatively long seismic quiescence, this region is now considered under high risk from a major megathrust earthquake and consequent tsunami that could strike the southwest coast of British Columbia (Dragert and Rogers, 1988). As part of natural hazard risk mitigation studies, several investigators have undertaken numerical computations of potential tsunamis originating from a megathrust CSZ failure along the North America coast (e.g., Ng et al., 1990, 1991; Whitmore, 1993). Investigations of CSZ tsunamis dramatically increased following reliable evidence of a M_w 9.0 megathrust earthquake and associated great trans-Pacific tsunami on 26 January 1700 that swept along the nearly 1000-km Pacific coast of Japan and led to intense flooding along the California, Oregon, Washington and Vancouver Island coasts (Atwater et al., 1995; Satake et al., 1996).

The purpose of this report is to present results of numerically simulated tsunami waves that could be generated by a CSZ earthquakes of M_w 9.0. Here, the goal is to examine the effects of global sea level rise over the next two centuries on tsunami waves arriving at Boundary Bay in the southern Strait of Georgia from a CSZ earthquake.

2. MODEL SETUP

2.1. Nested grid formulation

Accurate numerical simulation of tsunami waves in the rapidly shoaling regions of the west coast of British Columbia requires setting up the model domain as a series of nested grids of ever finer spatial and temporal resolution. The use of nested grids and nested-grid formulation is described in Fine et al. (2018). The parameters of the nested grids are presented in Table 1. The domains of Grids 1 through 4 for present-day mean sea level are shown in Figures 1 to 4, respectively.

Table 1. Parameters of the numerical grids used in the tsunami generation and propagation model. Grid extent is along the *x* (eastward) and *y* (northward) coordinate directions and is presented in degrees (°). Numerical grid cell sizes for Grids 2, 3 and 4 are roughly 270, 60 and 10 m, respectively. Columns 2, 3 and 4 are presented as *x*, *y* values. DEM denotes the Digital Elevation Model provided by Ocean Networks Canada. Note: 1° latitude = 60 nautical miles (~111 km).

Grid No.	Extent (*x*, *y*) (degrees)	Array (number of grid points)	Cell size (degrees)	Source of data	Processing type
1	18.0, 17.0	721, 1021	0.025, 0.01667	GEBCO 2014 30 arc-seconds gridded data	Filtering and bilinear interpolation
2	6.595, 4.2	1261,1520	0.005, 0.00333	BC 3 arc-sec bathymetric DEM	Filtering and bilinear interpolation
3	0.74, 0.55	811, 889	0.0008333, 0.0005555	BB 1/9 arc second DEM	Filtering and interpolation
4	0.38, 0.20	2737, 2161	0.000138889, 0.0000925926	BB 1/9 arc second	Filtering and interpolation

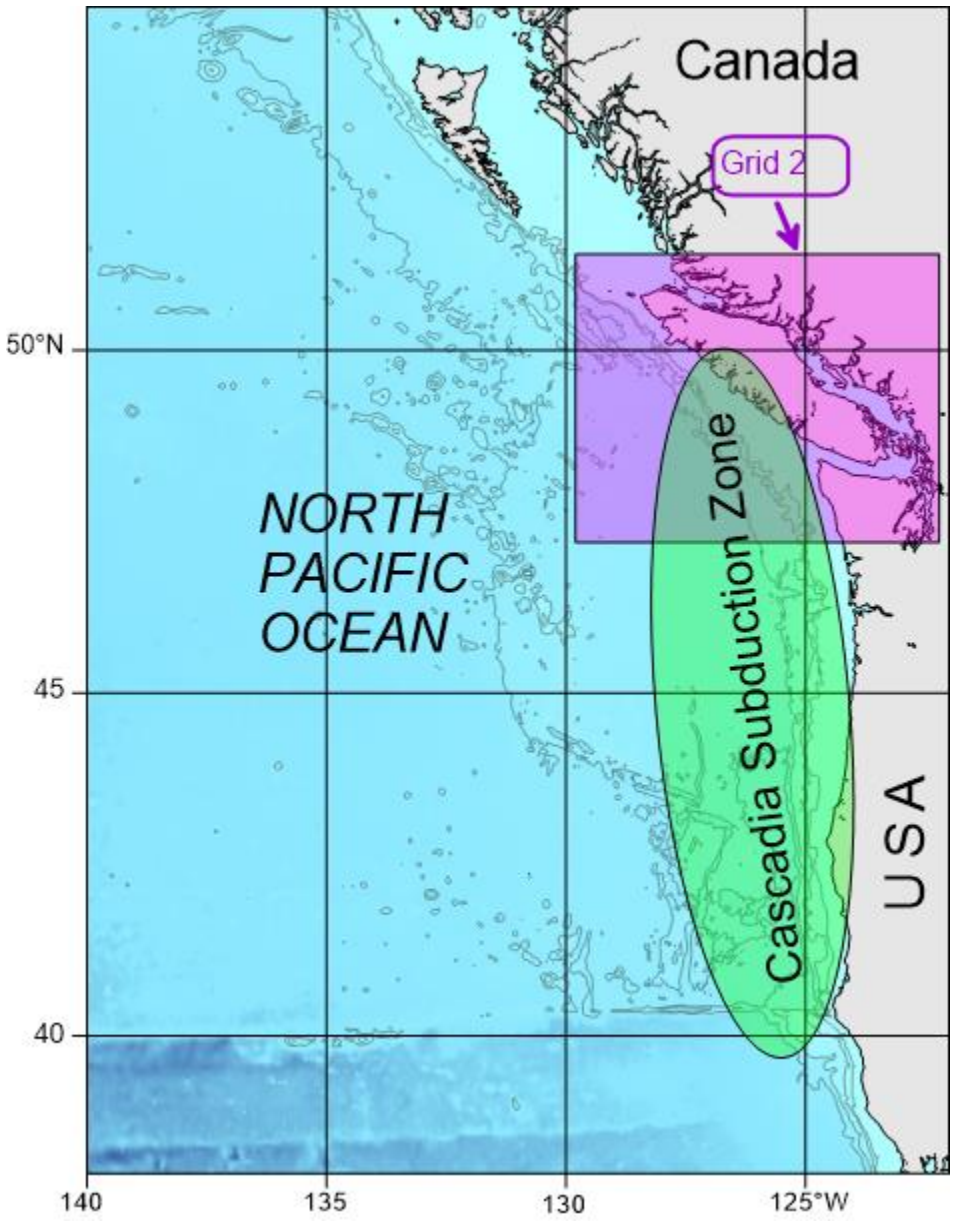

Figure 1. The region covered by the large-scale coarse grid numerical model for the northeast Pacific (Grid 1). Also shown is the Cascadia Subduction Zone where a tsunami could be generated that would impact the Boundary Bay area. The insert shows the location of the first nested grid (Grid 2), covering the southwest coast of British Columbia and northwest Washington State.

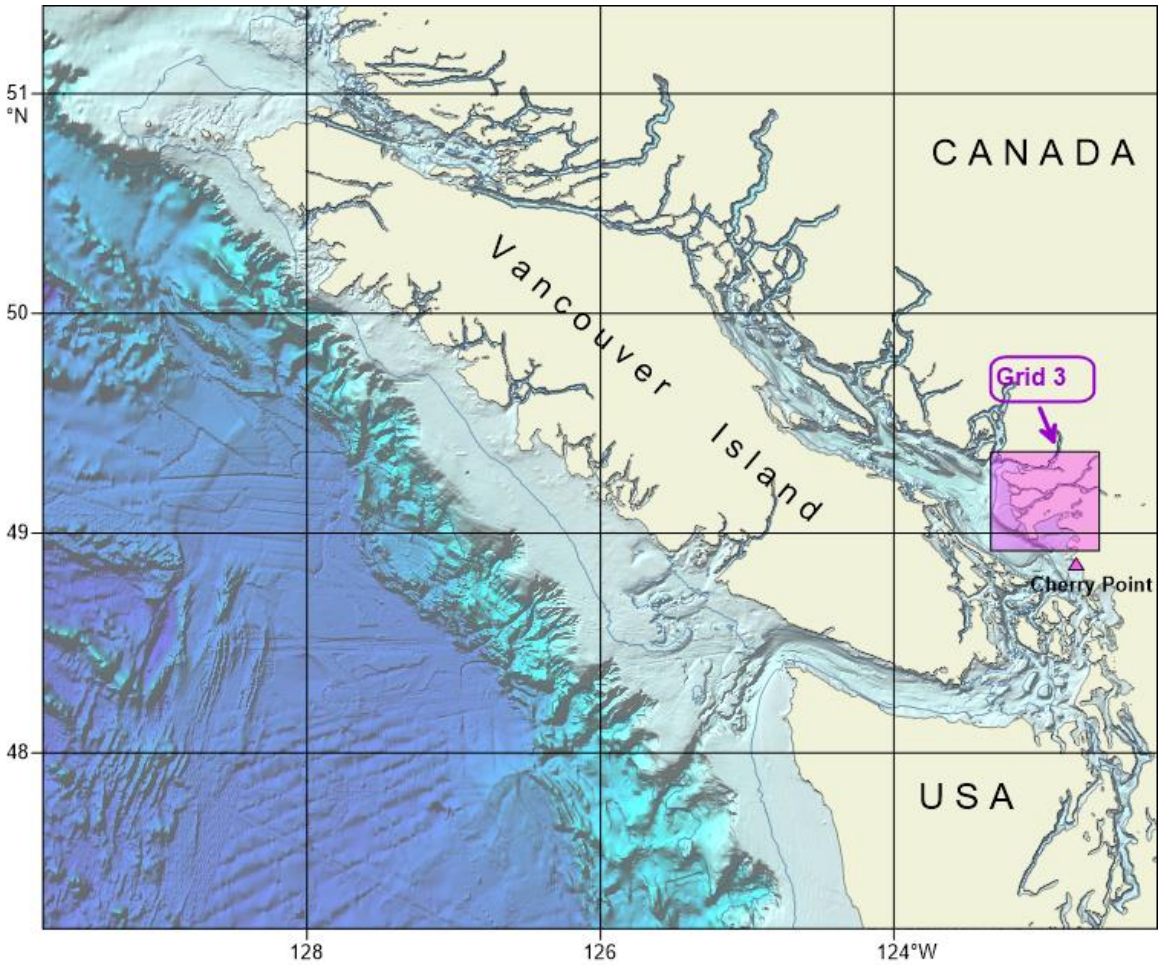

Figure 2. Vancouver Island and surrounding oceanic regions covered by the medium-scale bathymetric grid (Grid 2) for the southwest coast of British Columbia. The horizontal grid cell scales (x, y) for this region are approximately 370 m. The insert shows the boundaries and location of the second nested grid (Grid 3) covering the region of Vancouver and Boundary Bay.

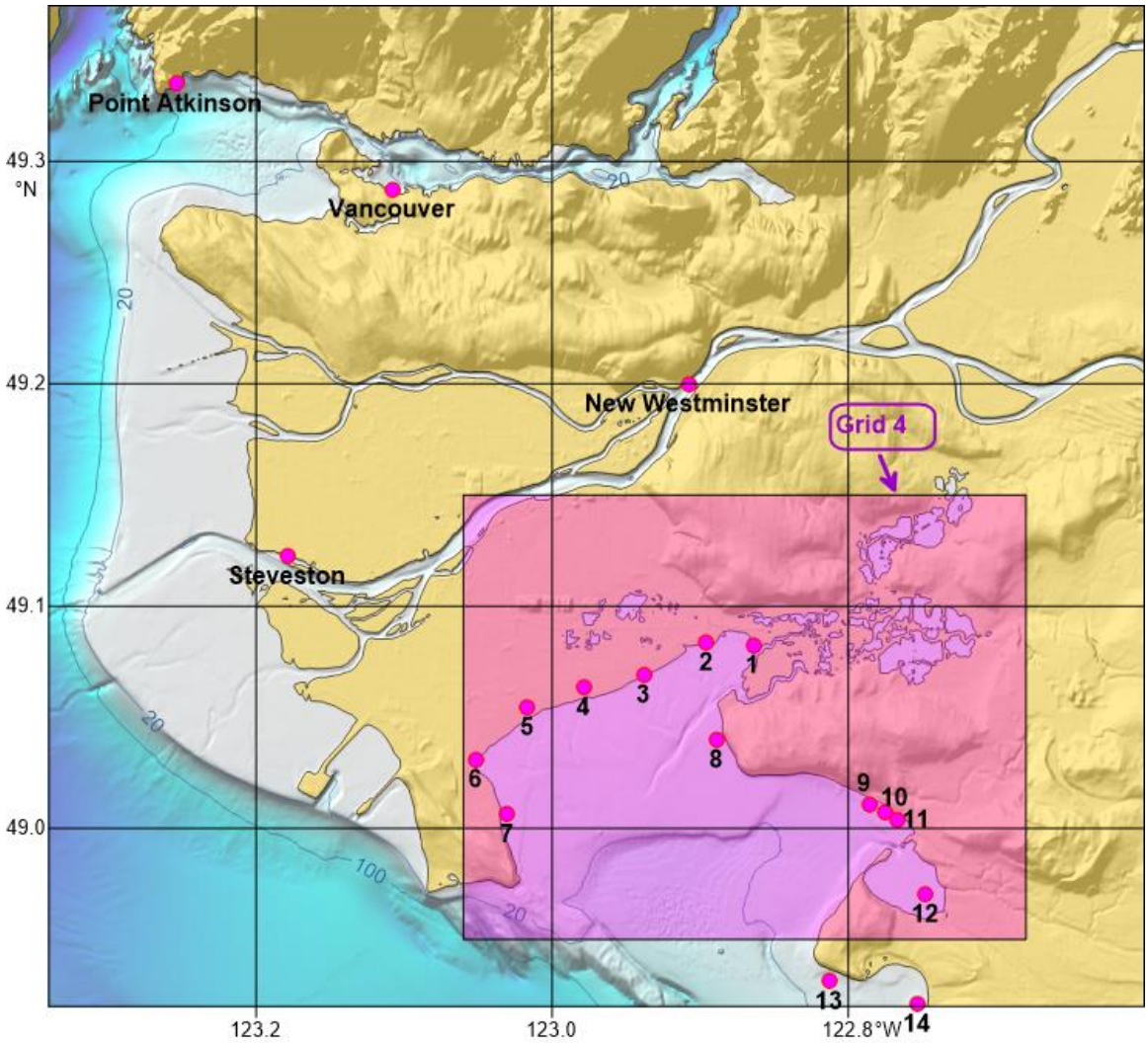

Figure 3. The coastal region covered by Grid 3, including the waters surrounding Greater (Metro) Vancouver. The *x*, *y* grid scales for this region are approximately 61 m and 62 m, respectively. Shown are the locations of the tide gauges (solid dots) and the modelled sites (numbers 1-14). The area above present-day mean sea level is shaded yellow. The insert shows the boundaries and location of the fourth nested grid (Grid 4) covering Boundary Bay.

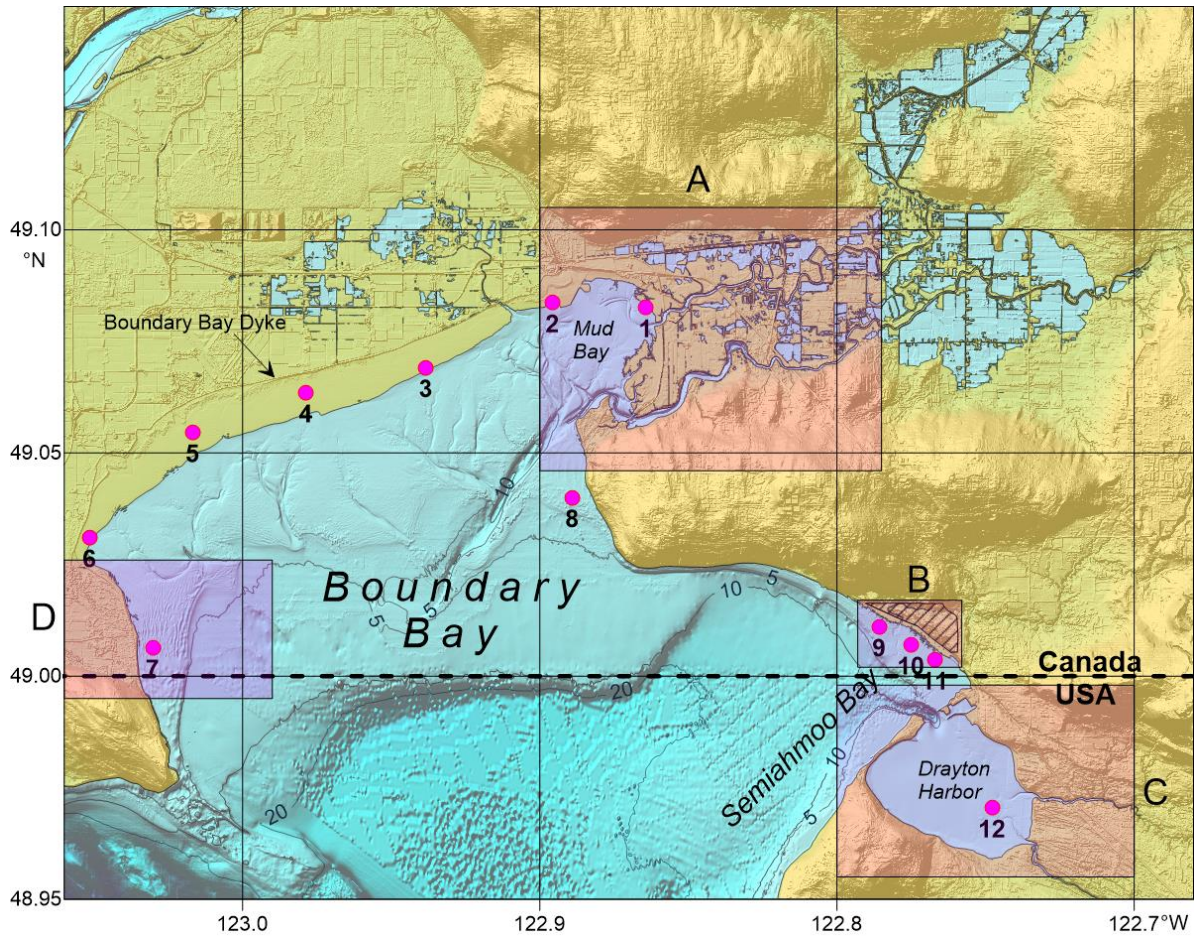

Figure 4. The region covered by Grid 4. The fine-scale bathymetric grid has adjusted topography for Boundary Bay, with grid scales (x, y) of approximately 10 m by 10 m. Also shown are the sites (numbers 1-12) for which tsunami wave records have been simulated. Depths, H, are in metres (m). The area above present-day mean sea level is shaded in yellow. The hatched area denotes the location of the Semiahmoo, First Nations. The 5, 10 and 20 m depth contours have been labelled.

2.2. Sea level rise scenarios

We have considered three scenarios of sea level rise derived initially from the Fifth Assessment Report of the Intergovernmental Panel on Climate Change (Stocker et al., 2013):

a. *Scenario-1 (S1)*: The Median RCP8.5 scenario, which leads to an approximately 0.5 m rise in global sea level by 2080;

b. *Scenario-2 (S2)*: The Upper RCP8.5 scenario, which leads to an approximately 1 m rise in global sea level by 2100;

c. *Scenario-3 (S3)*: Extreme global sea level rise of 2 m by year 2200.

Details on the above scenarios are described in the **"***Tabulated Values of Relative Sea-Level Projections in Canada and the Adjacent Mainland United States"* (Geological Survey of Canada, Open File 7942, 2015). The digital data of sea level rise for the present study were downscaled into a nested grid model.

Maps of sea level rise for the three scenarios for Grid 2 of the modeled domains are shown in Figure 5. The distributions consist of sea level rise minima in the northern Strait of Georgia, as well as in the central and southern parts of the west coast of Vancouver Island. The highest rise is in the southern Strait of Georgia and eastern Juan de Fuca Strait. Differences in sea level rise are related to differences in local tectonic uplift.

Figures 6 and 7 show further downscaling of the original sea level rise values into the level 3 and level 4 modeling domains. It is clear that for sea level rise Scenario-2 (corresponding to a 1 m global sea level rise), parts of Greater Vancouver will be below mean sea level. The situation is even more serious for Scenario-3, where significant parts of the area will be below mean sea level and will need protection.

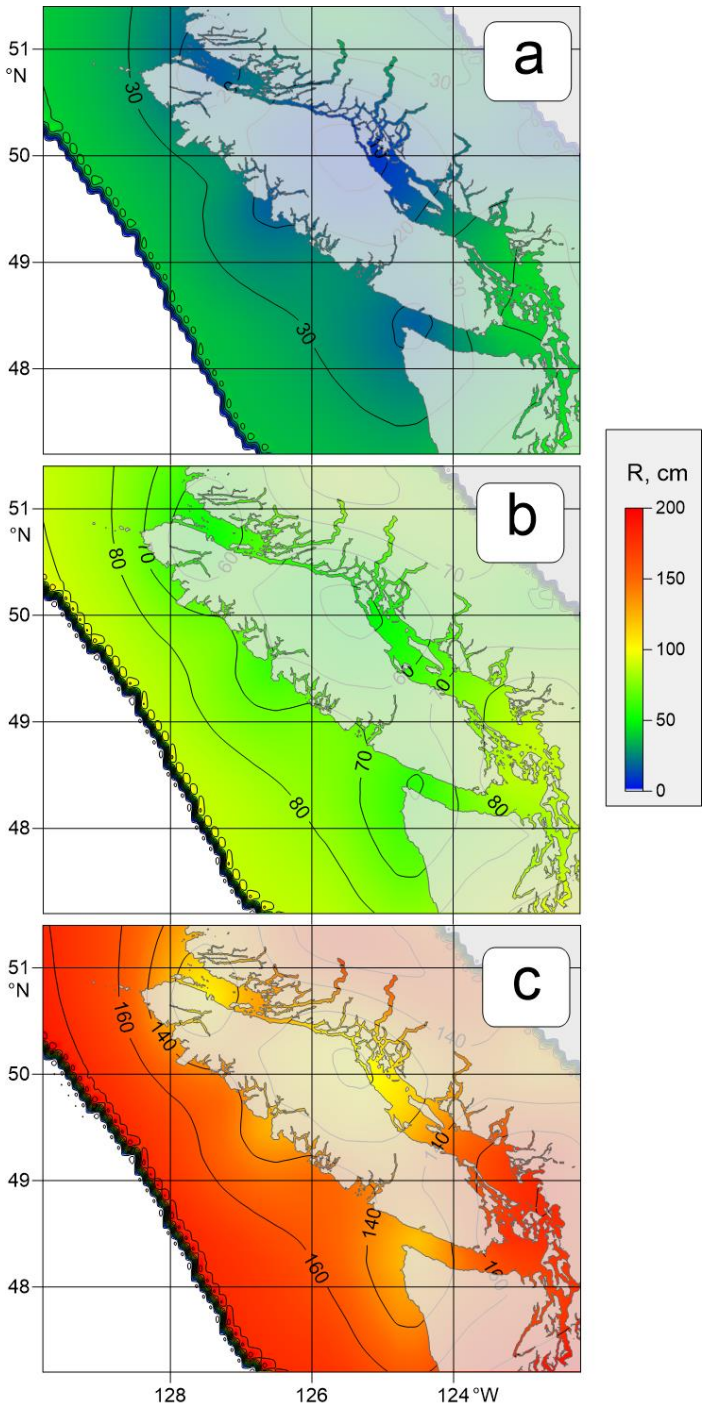

Figure 5. Sea level rise (R, cm) distributions over the domain of Grid 2 of the model for: (a) a 0.5 m global rise for the median RCP8.5 (Scenario-1; S1); (b) a 1 m global rise for the upper RCP8.5 (Scenario-2; S2); and (c) a 2 m global rise for the year 2200 (Scenario-3; S3).

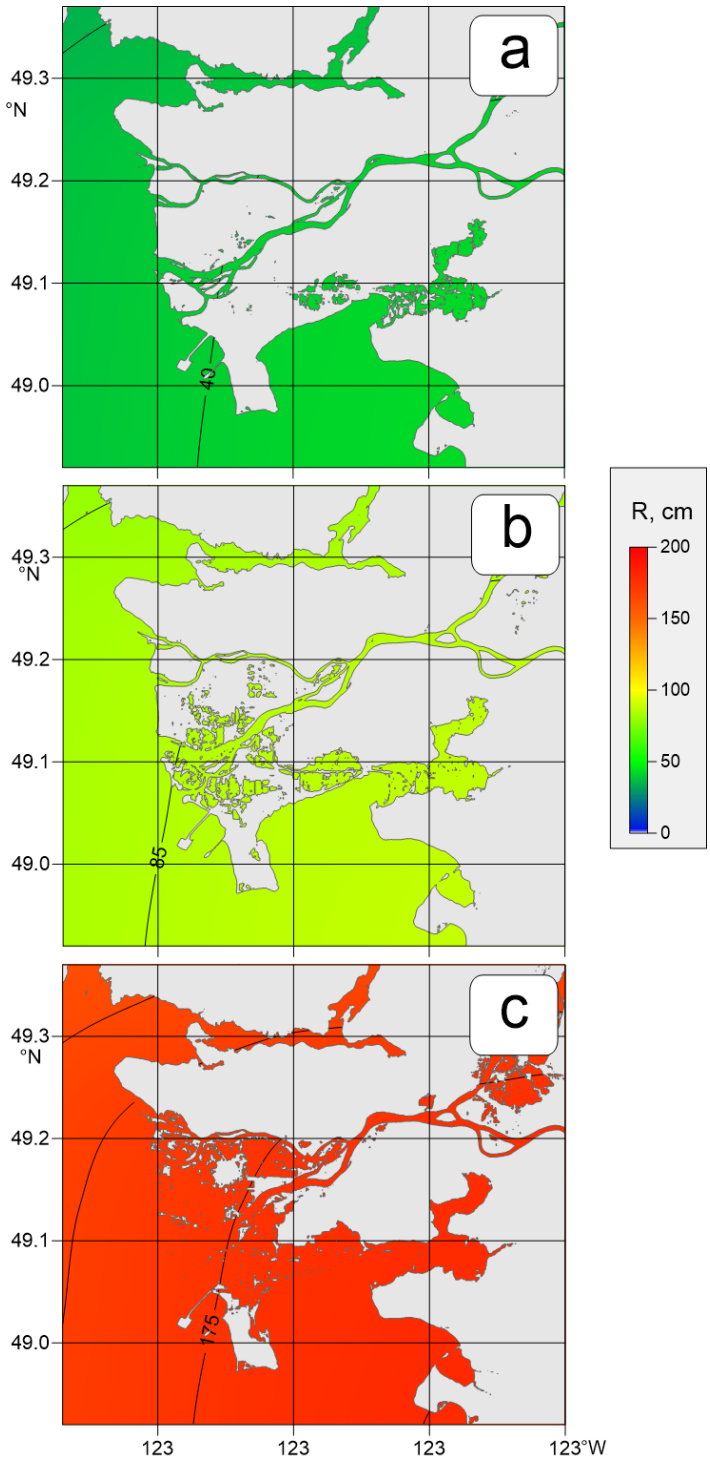

Figure 6. Sea level rise (R, cm) distributions over the domain of Grid 3 of the model for: (a) a 0.5 m global rise for the upper RCP8.5 (Scenario-1); (b) a 1 m global rise for the upper RCP8.5 (Scenario-2); and (c) a 2 m global rise for the year 2200 (Scenario-3). The land area lying above mean sea level is shown in grey.

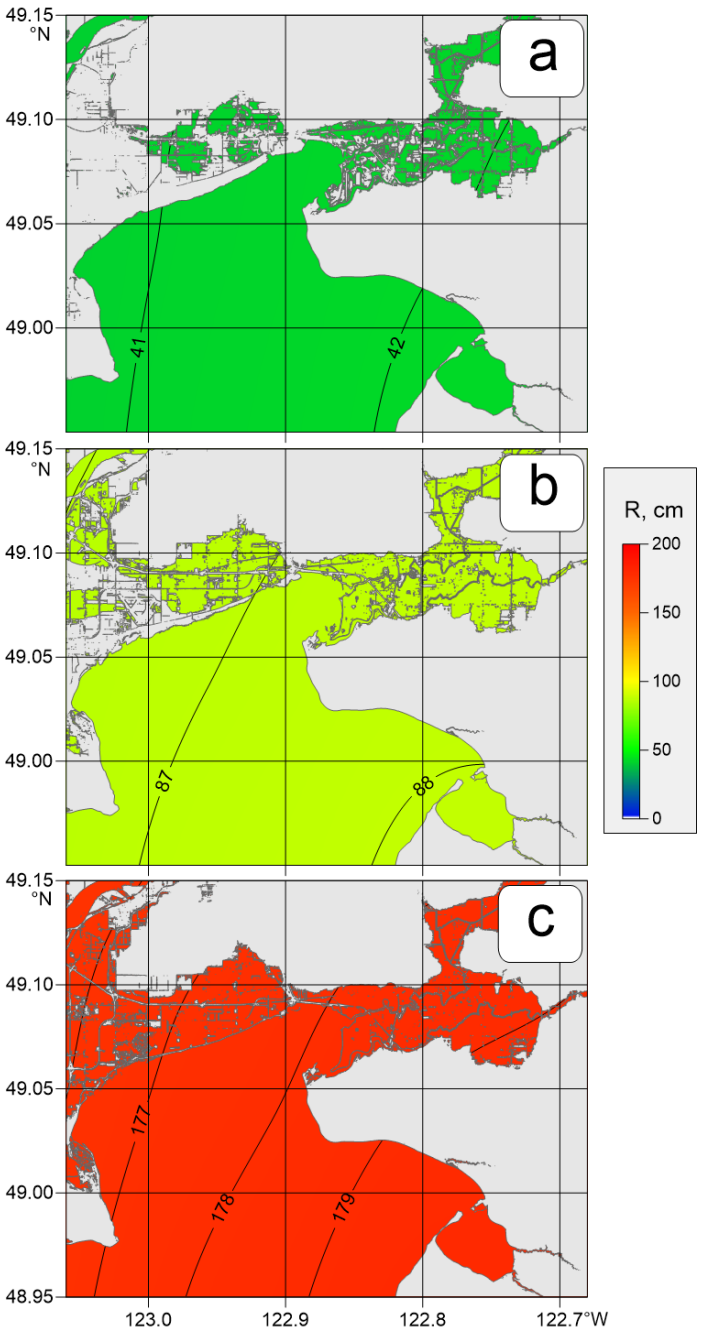

Figure 7. Sea level rise (R, cm) distributions over the domain of Grid 4 of the model for: (a) a 0.5 m global rise for the median RCP8.5 (Scenario-1); (b) a 1 m global rise for the upper RCP8.5 (Scenario-2); and (c) a 2 m global rise for year 2200 corresponding to (Scenario-3). The land area lying above mean sea level is shown in grey.

2.3. Dike Height in Boundary Bay

The shores of Boundary Bay are presently protected from flooding by a dike situated along the north-eastern side, around the northern coast, and along the north-western to the eastern coastline. The dikes, which protect low land in the coastal area, can be divided into three zones (Figure 8). In Zone A, the top of the dike is currently about 3 m above geodetic datum (see Figures 9 and 10). In Zone B, the northern segment, the top of the dike is roughly 3.5 m above geodetic datum (see Figures 9 and 11). Finally, in the north-western segment (Zone C), there is a series of dikes, which protect the land to the northwest of Boundary Bay from direct flooding from the Bay, and from two rivers, the Serpentine and Nicomekl, whose shores are also protected with dikes on both sides of the rivers. Zone C is the most complicated area and the heights along the tops of the dikes vary considerably, from 2.8 m to nearly 5 m above geodetic datum (see Figure 12 for cross-sections and Figure 9 for a map of the dike).

It is apparent from the results for Scenario-2 (sea level rise for the upper case of RCP8.5 by 2100) that the current dike level only marginally protects low-lying areas, as the maximum tidal level (Large Tide) is about 60-65 cm above higher high water mean tide (HHWMT). In the case of Scenario-3, even the HHWMT level will be above the present level of the dike. As a consequence, the model cannot start normally for future sea level conditions as flooding will begin at the start of the model run, well before any tsunami waves arrive in the area.

To avoid initial flooding, we raised the top of the dike in our model by about 1.5 m. The dike-rise procedure was performed in three stages. During the first sage, the existing dike axis (the line marking the top of the dike) was digitized using special software having an accuracy of the order of the grid size (about 10 m). During the second stage, a moving “dump truck” algorithm was applied, with small horizontal steps of about 1 m for each increment along the dike path. Starting by raising the end of the dike by 1.5 m, the algorithm raises the dike by artificially adding “material” (i.e., adding elevation) to the top of the dike. At each 1-m step, the algorithm creates a new dike topography having the shape of a round 2D Gaussian distribution with a height of 1.5 m and its centre at the current position on the dike path. The Gaussian radius was set to 40 m. The Gaussian height at the new position was then compared to the modified dike height at the previous step. A new Gaussian shape was then created at the new site by allocating to the new site the highest value of the previously constructed height and the current site. Then the “dump truck” was advanced along the dike path to

the next location. Finally, a near-ideal “upgraded” dike with a uniform height was created along the whole path. The upgraded dike heights are shown as dashed lines in Figures 10 to 12.

Finally, at the third stage, the upgraded dike bathymetry was added to the existing model bathymetry to create an updated bathymetry for Grid 4 for future modeling use. Figures 10, 11, and 12 shows the existing and updated cross-section of the bathymetry along different lines.

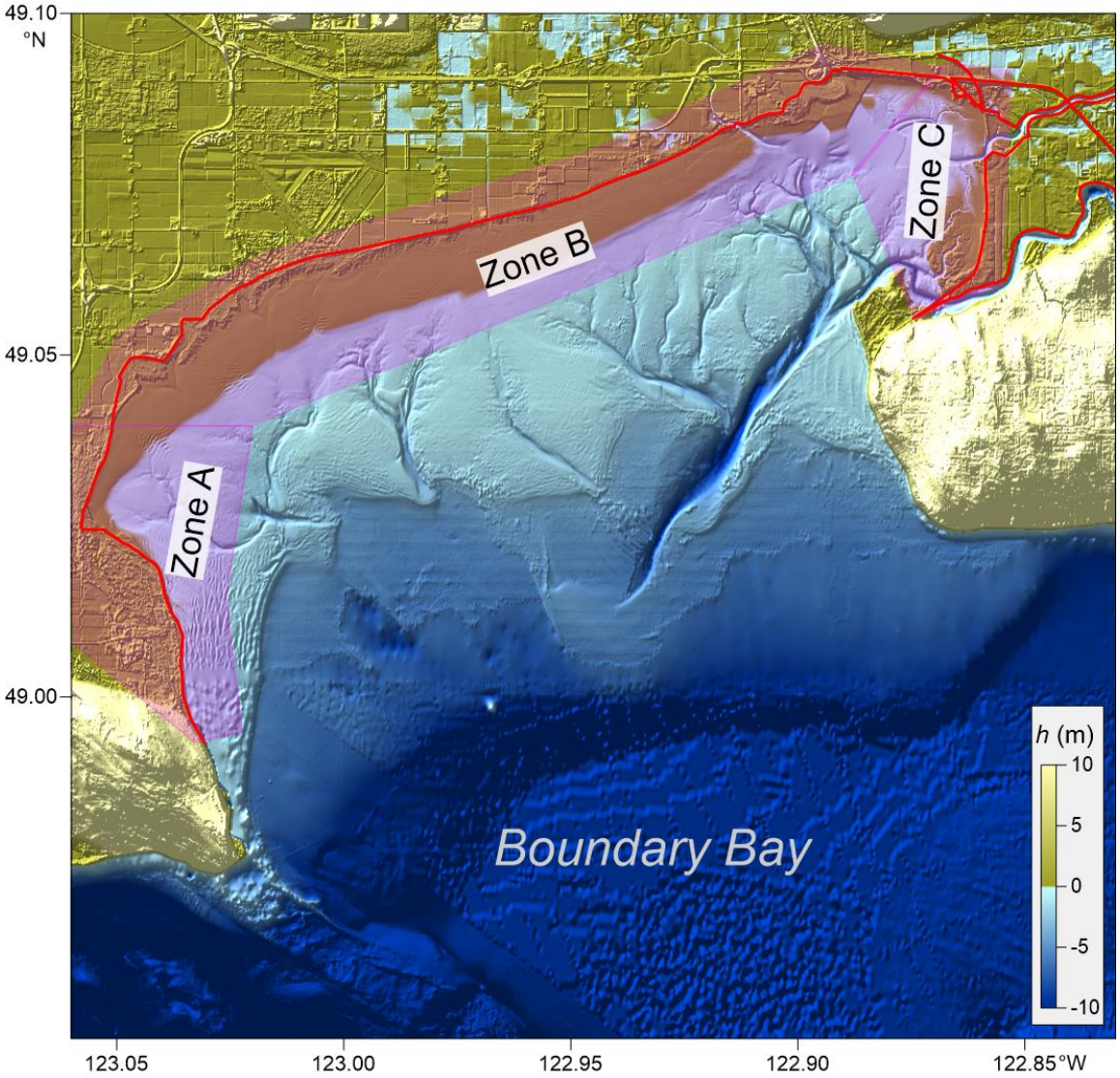

Figure 8. Map of Boundary Bay created using the bathymetric map for the Grid 4 domain. Shown are the locations of the dikes and the dike zones. Here, *h* denotes the land elevation (positive values) and the water depth (negative values in blue).

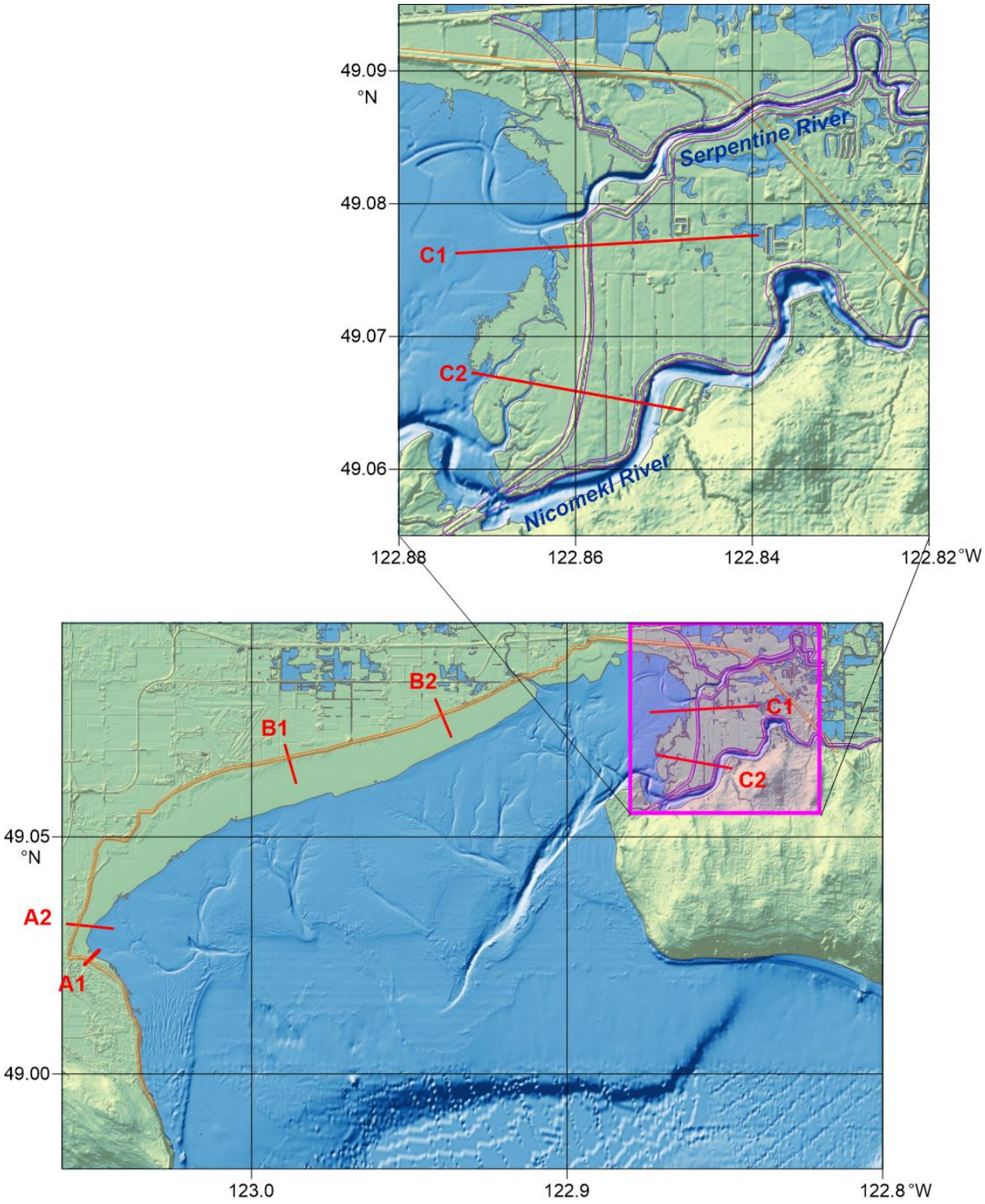

Figure 9. Map of Boundary Bay showing the locations of the dikes and locations of cross-sections across the dike applied in the model. The insert shows the location of the dikes along the rivers. (see Figures 10 to 12.)

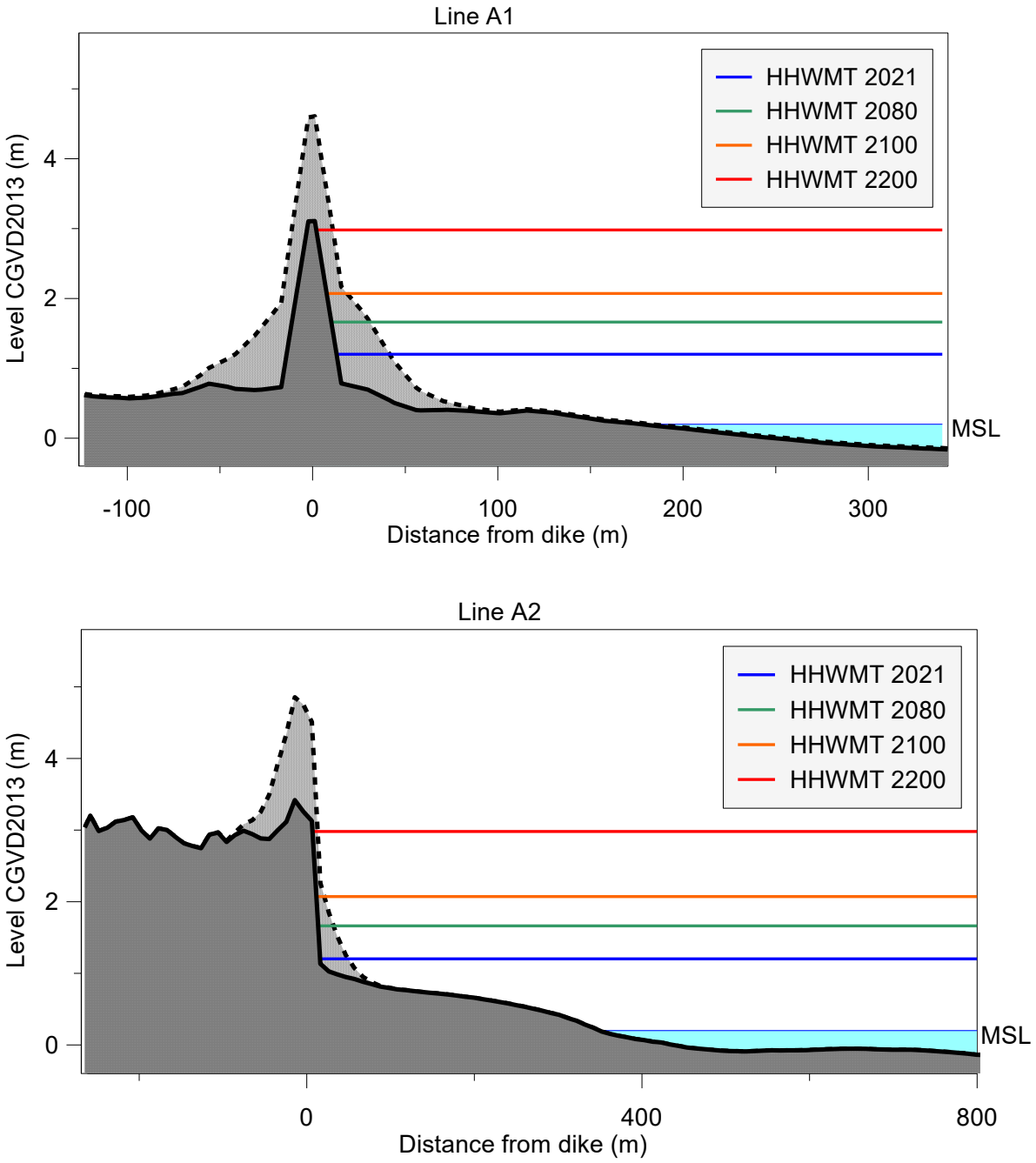

Figure 10. Cross-sections along lines A1 (upper panel) and A2 (lower panel). See Figure 9 for the locations of the lines. Also shown are the positions of present-day higher high water mean tide (HHWMT) (blue lines) and HHWMT for different sea level rise scenarios. The solid line and darkly shaded region denote the existing seabed and dike; the dashed line and lightly shaded region denote a proposed future dike. CGVD 2013 denotes the Canadian Geodetic Vertical Datum.

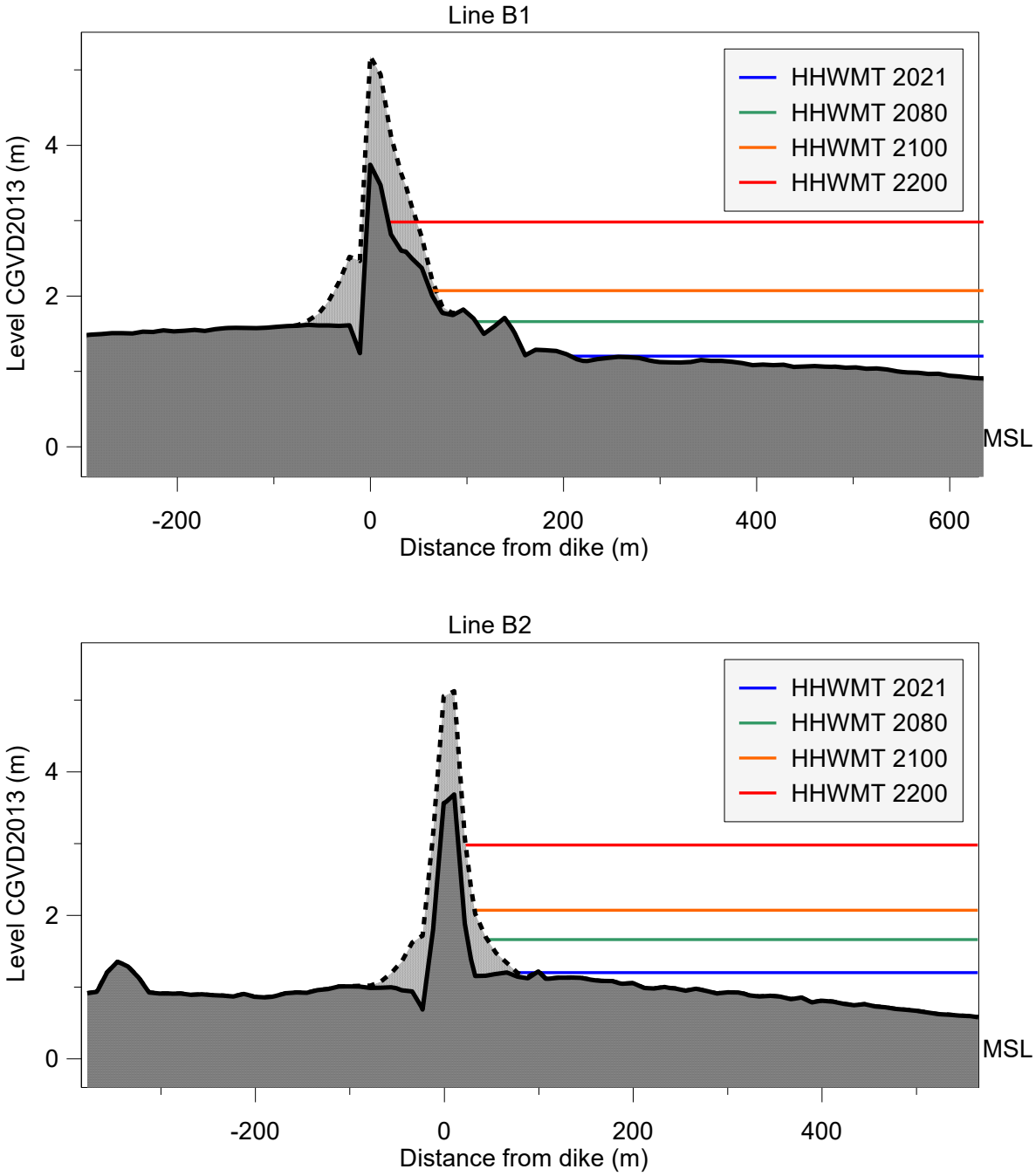

Figure 11. Cross-sections along lines B1 (upper panel) and B2 (lower panel). See Figure 9 for the locations of the lines. Also shown are the position of the present-day higher high water mean tide (HHWMT) (blue lines) and HHWMT for different sea level rise scenarios. The solid line and darkly shaded region denote the existing seabed and dike; the dashed line and lightly shaded region denote a proposed future dike. CGVD 2013 denotes the Canadian Geodetic Vertical Datum.

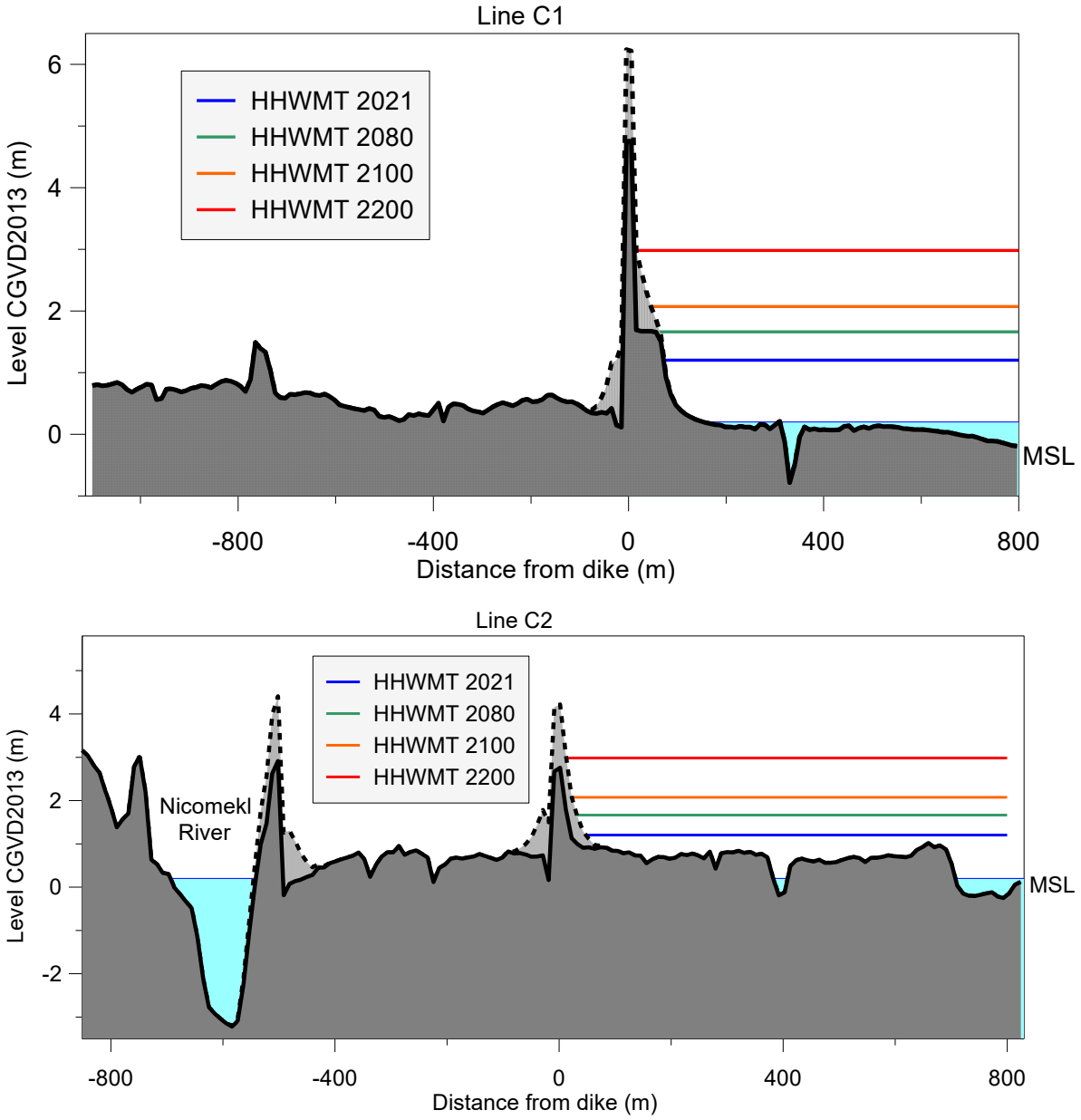

Figure 12. As for Figure 11 but for lines C1 (upper panel) and C2 (lower panel). CGVD 2013 denotes the Canadian Geodetic Vertical Datum.

2.4. Model reference level

Model simulations are typically conducted for tsunami arrival times that coincide with times of the Canadian Vertical Datum for higher high water mean tide (HHWMT). The National Tsunami Hazard Mapping Program of 2010 (Nikolsky et al., 2013) recommends that inundation maps be computed using high tide as the initial condition for modelling. Alaska University uses Mean Higher High Water (MHHW) as the initial condition (Suleimani et al., 2013), while the Washington State inundation map was created using Mean High Water (MHW) for the initial conditions (Eungard et al., 2018. The Canadian standard HHWMT is close to the US standard MHHW and has been used for many tsunami modelling projects in BC, including for Victoria (AECOM, 2013), for Victoria and Seal Cove (Fine et al., 2018), and for Prince Rupert (The City of Prince Rupert Tsunami Flooding Risk Assessment, 2019). Accordingly, to present values of highest risk, maps of maximum tsunami wave height and current speed in this report are referenced to HHWMT rather than to the mean tide or to a geodetic reference.

Higher High Water Mean Tide (HHWMT) is used as the primary reference level for most modelling results. For the Boundary Bay area, the closest permanent tide gauges are at Point Atkinson and Vancouver (Canadian Hydrographic Services) to the north and Cherry Point (NOAA) to the south. HHWMT is 1.30 m above Mean Sea Level (MSL) at Point Atkinson and 1.32 m above MSL at Vancouver; in comparison, MHHW used in the US is 1.18 m above MSL at Point Atkinson (see Table 2 below). For convenience, a common reference value of 1.2 m is added throughout the region for the tsunami modelling. Mean Sea Level (MSL) is 0.18-0.19 m above the Canadian geodetic datum CVD2013 (Table 2).

For each of the three sea level rise scenarios, the computed sea level rise values for each grid (see Figures 5-7) were added to the bathymetry of Grids 2, 3 and 4, in addition to the Higher High Water values. Grid 4 has a modified dike, whose height was increased by 1.5 m (see Section 2.3 for details). Grid 1 was unchanged.

Table 2. Vertical datum values for tidal stations provided by the Canadian Hydrographic Service (CHS) and the US National Oceanic and Atmospheric Administration (NOAA). Latitude and longitude are in degrees and minutes. Mean Higher High Water (MHHW) and Mean Lower Low Water (MLLW) are defined in two ways: (1) in Canada using tidal predictions derived from tide gauge records; and (2) in the United States using observations from USA tide gauges. All values are referenced to Mean Sea Level (MSL), which by definition in this study is then zero (0.0). Here, CGVD 2013 denotes the Canadian Geodetic Vertical Datum.

Tide gauge ID	Station	Latitude (°N)		Longitude (°W)		CGVD 2013	MSL	MHHW	MLLW
		Deg	Min	Deg	Min	(m)	(m)	(m)	(m)
7795	Point Atkinson	49	20.25	123	22.42	-0.193	0.0	1.30	-1.94
7735	Vancouver	49	17.23	123	6.587	-0.180	0.0	1.32	-1.96
9449424	Cherry Point	48	51.80	122	45.5	-	0.0	1.18	-1.61

2.5. The source distribution

A detailed characterization of megathrust rupture models used for simulating tsunami inundation was presented recently by Gao et al. (2018). The authors examined 15 megathrust earthquake scenarios, with emphasis on two main scenarios, a buried rupture and a splay rupture.

In this study, we use a version of the buried rupture model. As shown previously (Fine et al., 2018), a splay scenario provides higher runup values along the west coast of Vancouver Island, while in the Strait of Georgia, a buried scenario produces slightly higher tsunami waves than the splay rupture scenario. A previous modeling study of the CSZ tsunami in Boundary Bay confirms this result (Fine et al., 2023). As a result, we restrict our attention to the buried rupture model as the worst-case scenario for the Boundary Bay area. The co-seismic vertical deformation for this scenario is shown in Figure 13.

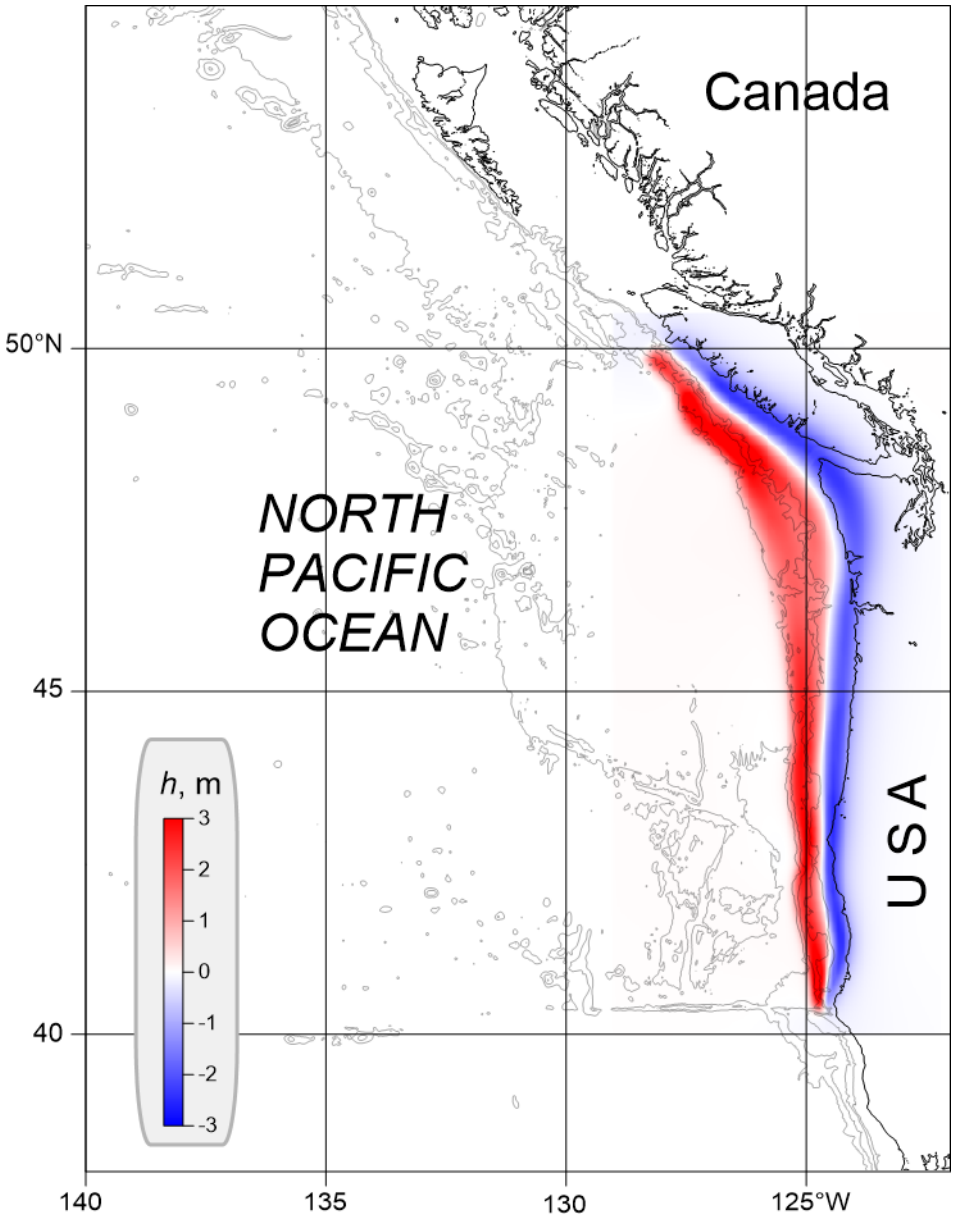

Figure 13. Seafloor vertical displacements (*h*, m) at the source region for a magnitude 9.0 Cascadia Subduction Zone (CSZ) buried earthquake tsunami from Gao et al. (2018). Seafloor displacements range from roughly -3 m (blue) to +6 m (red); the scale in the legend has been truncated at +3 m in order to highlight the spatial gradation in the lower values.

3. RESULTS

3.1. Maximum tsunami wave heights for the coarse and intermediate grids

The computed distributions of wave height maxima for a future CSZ tsunami based on grids 1-3 are presented in Figures 14-18. Figure 14 shows the distribution of the maximum tsunami wave heights for the entire northwest coast of North America, from California in the south to British Columbia in the north. While tsunami wave-height maxima are found along the coastal zone, considerable tsunami energy is radiated to the southwest off the west coast. In British Columbia and along the US West Coast, the most affected coastal zones are those exposed to the open ocean, such as the west coast of Vancouver Island and the west coast of Washington and Oregon States. In more protected areas, such as Juan de Fuca Strait, the computed tsunami wave amplitudes are markedly smaller (Figure 15; Grid 2). The results for Grid 2 are similar for all three sea level rise scenarios.

Results for the finer resolution grids (Grid 3) demonstrate the considerable spatial variability in the incoming tsunami wave heights for the study region. Figure 16 shows the distribution of the tsunami wave heights for Grid 3 in the southern Strait of Georgia off Metro Vancouver for the 0.5 m sea level rise scenario (S1). As the figure indicates, wave amplitudes are much higher in Boundary Bay than near Vancouver to the north. Waves increase toward the shoreline and are especially high in the upper part of Boundary Bay and in Drayton Harbor (see Figure 17 for location). The pronounced increase in tsunami wave heights in the harbour is related to resonance amplification of the incoming tsunami waves.

For scenarios S2 and S3, corresponding to 1 m and 2 m global sea level rises, respectively, the amplitudes of the waves are generally smaller than the amplitudes for Scenario-S1. The decrease in tsunami amplitudes for the higher sea level rise scenarios is due to an increase in flooding in the lowlands of the Greater Vancouver region, which, in turn, is not related to inundation by the tsunami waves but to the initial water depth condition (see Figure 6 and Figure 7). The effect of the initial flooding of the low laying area in Boundary Bay was corrected for the final grid (see next section).

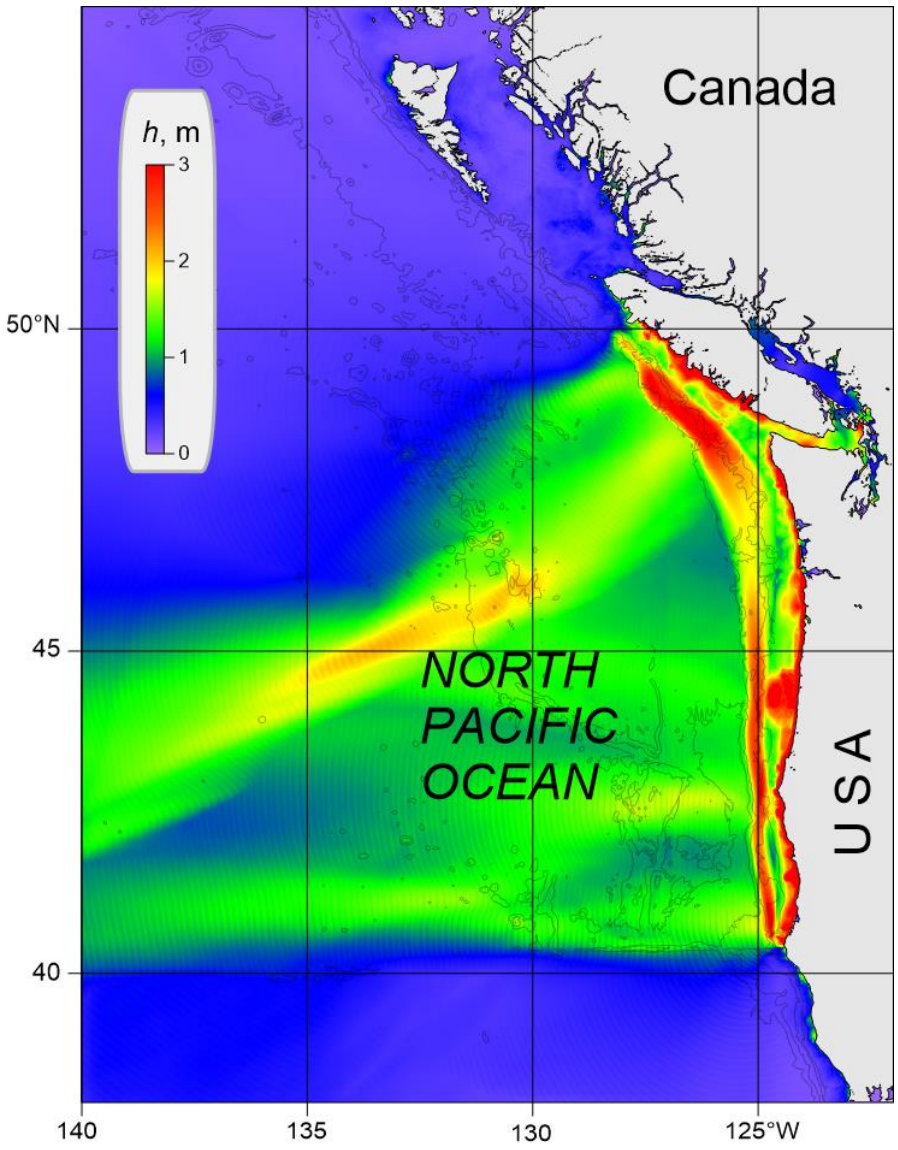

Figure 14. Distribution of the maximum tsunami wave heights (*h*, metres) for Grid 1 of the nested-grid model for waves generated by simulation of an earthquake-magnitude 9.0 CSZ tsunami (buried rupture source).

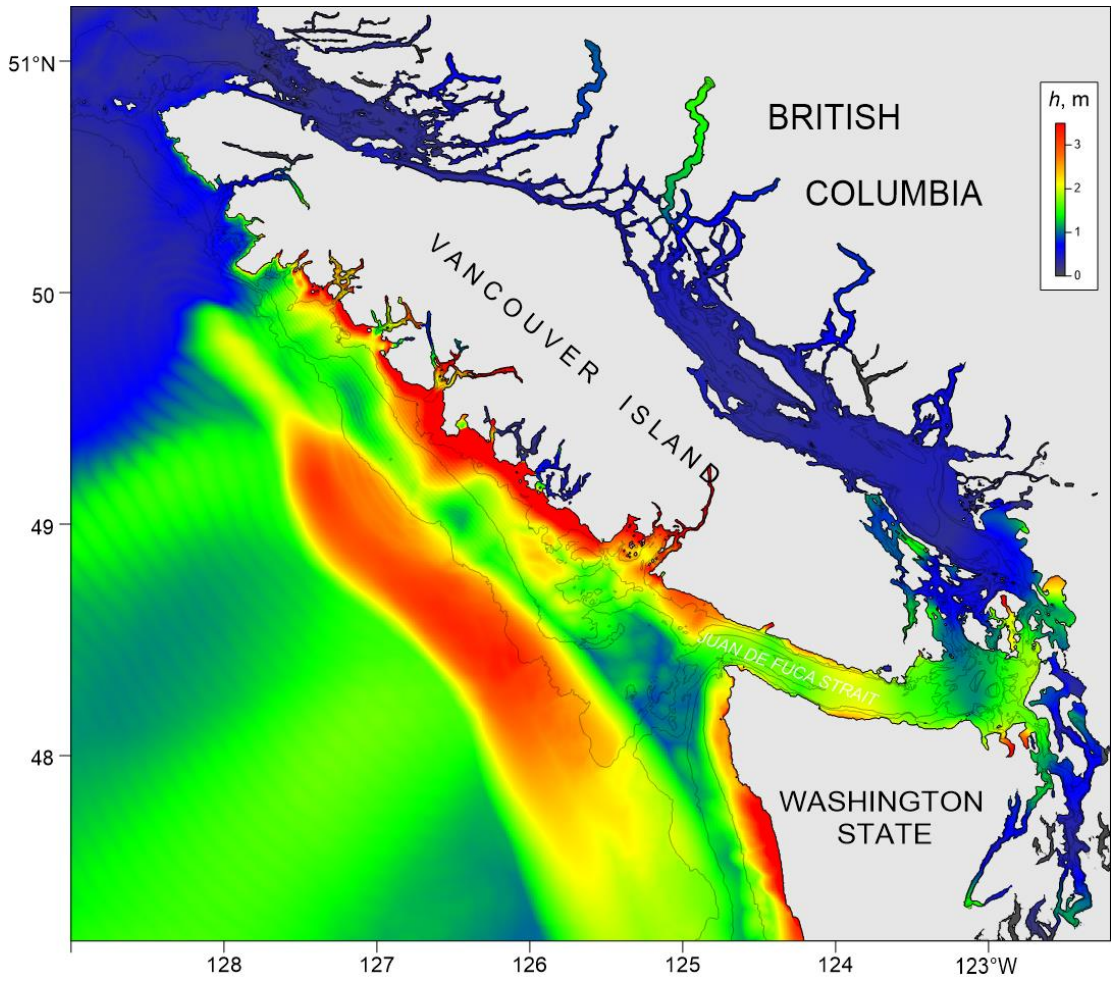

Figure 15. Distribution of the maximum tsunami wave heights (*h*, metres) for Grid 2 of the nested-grid model for waves generated by simulation of an earthquake-magnitude 9.0 CSZ tsunami from a buried rupture source with sea level rise for Scenario-3 (a global 2 m sea level rise by 2200).

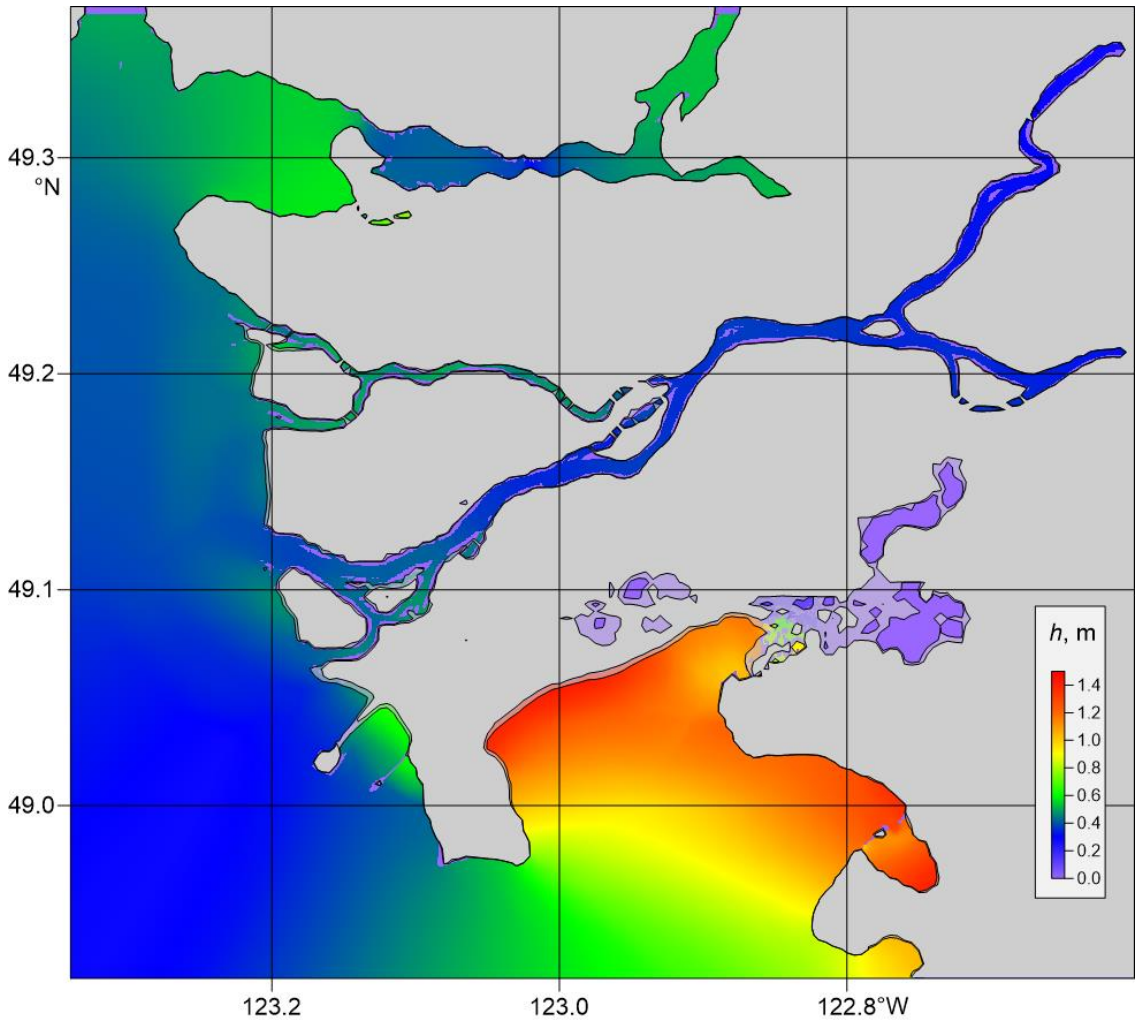

Figure 16. Distribution of the maximum tsunami wave heights (*h*, metres) for Grid 3 of the nested-grid model for waves generated by simulation of an earthquake-magnitude 9.0 CSZ tsunami for Scenario-1 (a global sea level rise of 0.5 m).

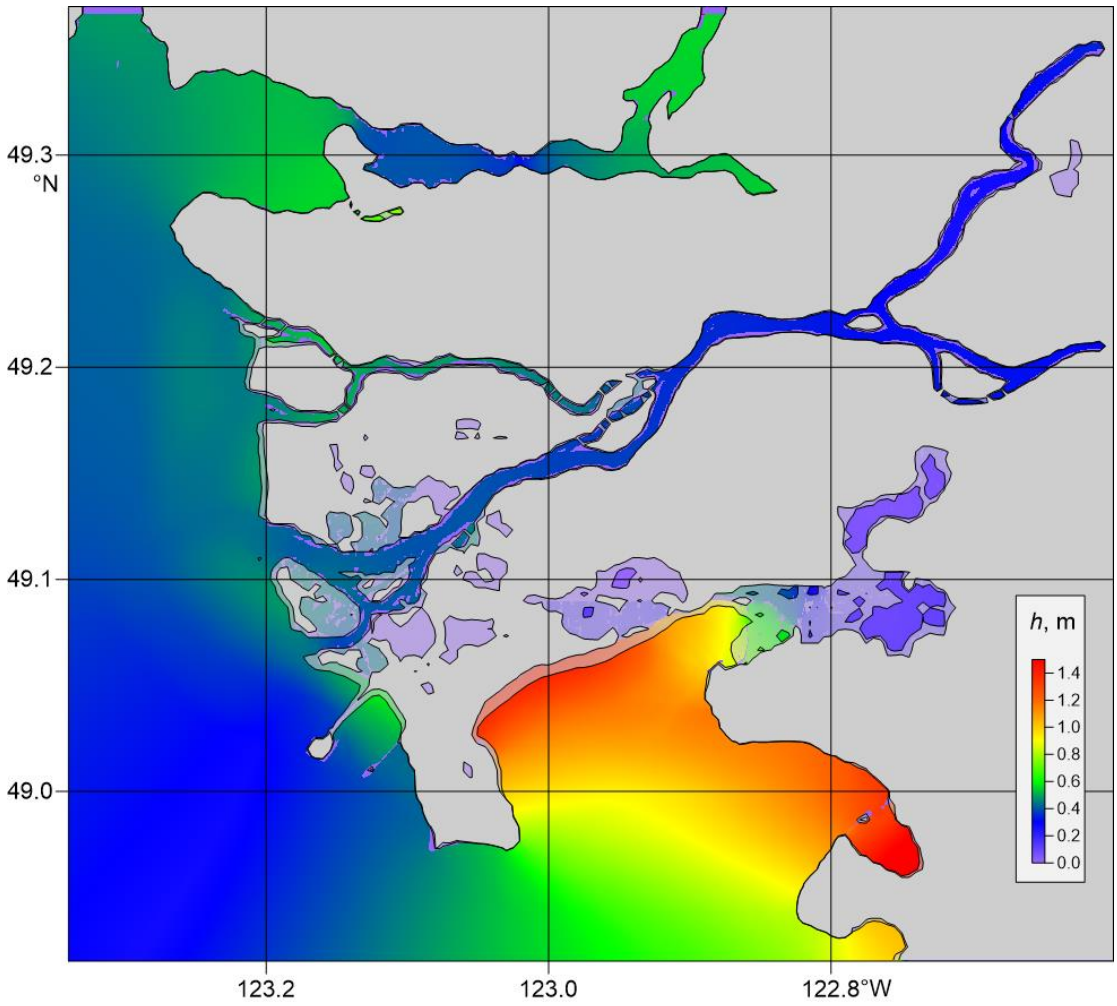

Figure 17. Distribution of maximum tsunami wave heights (*h*, metres) for Grid 3 of the nested-grid model for waves generated by simulation of an earthquake-magnitude 9.0 CSZ tsunami for Scenario-2 (global sea level rise of 1 m).

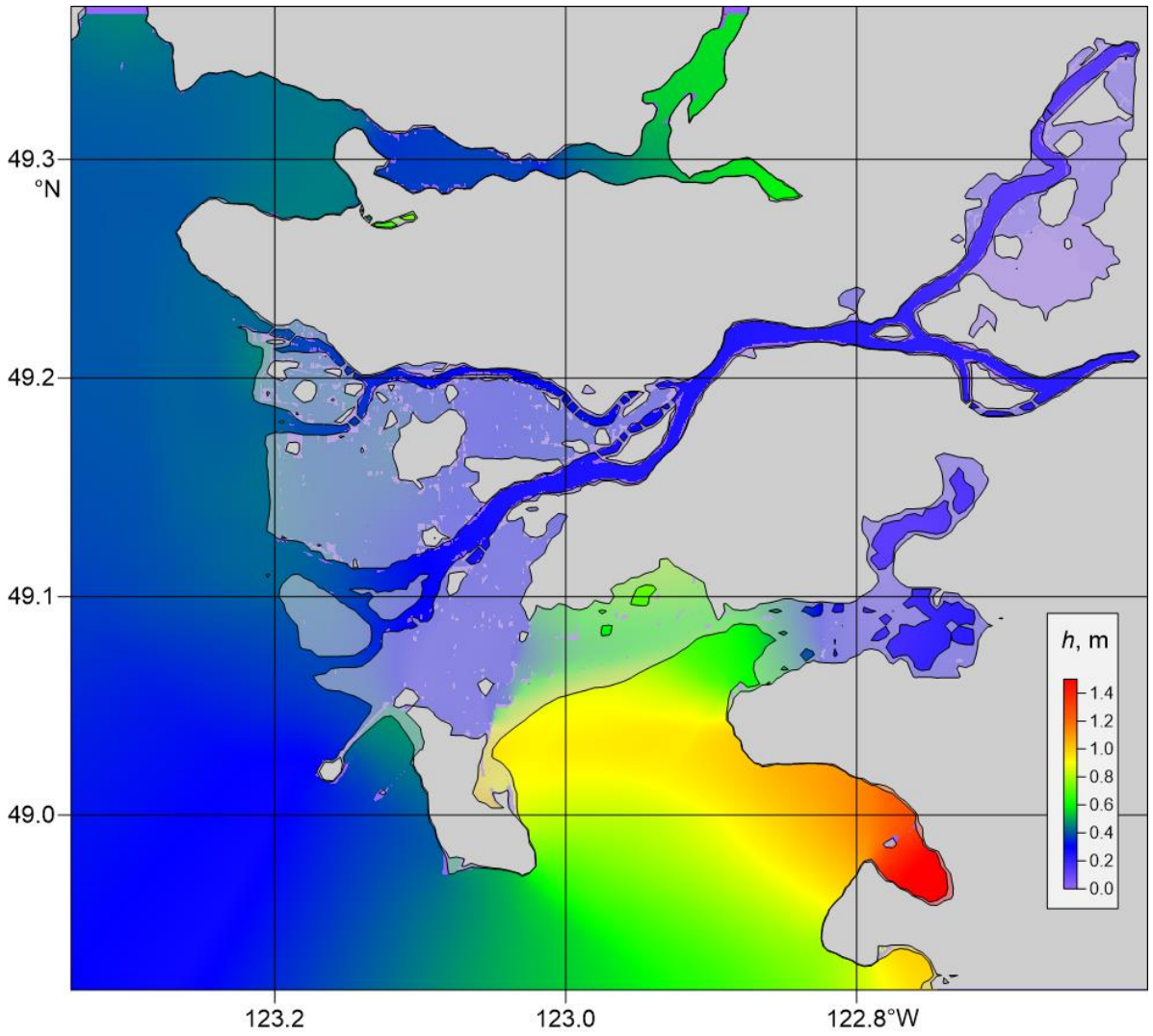

Figure 18. Distribution of maximum tsunami wave heights (*h*, metres) for Grid 3 of the nested-grid model for waves generated by simulation of an earthquake-magnitude 9.0 CSZ tsunami for Scenario-3 (global sea level rise of 2 m).

3.2. Detailed results for Boundary Bay: Tsunami wave heights and currents for different sea level rise scenarios

3.2.1. Wave heights

The tsunami waves for all three sea level rise scenarios were computed using the modified dike along the northern and eastern sides of Boundary Bay (Grid 4 domain), negating the possibility of any spill of water from outside the region at the time of the initial conditions. Also, we prohibited water from entering through the northwestern part of Grid 4 by requiring that other low-laying areas of Greater Vancouver were also protected (numerically at least) from the rising sea. In addition, we consider a case for Scenario-1 (0.5 m global sea level rise) with the current (non-modified) dike in place, to estimate the effect of a modified dike on the tsunami wave and on the inundated area.

Figure 19 presents a high-resolution map showing the distribution of the maximum tsunami heights in Boundary Bay and vicinity for Scenario-1 (global sea level rise of 0.5 m). For both cases, without (a) and with (b) updating of the dike, the wave amplitudes are similar and almost undistinguishable. However, in case (a) (i.e., with the current dike system), some areas in the eastern and western parts of Boundary Bay would be flooded by the tsunami, while our updated dike would protect all of these areas from flooding. The water depth in the flooding areas will generally be shallow, a few tens of centimeters only.

Results for the other scenarios are generally similar. Figures 20 and 21 show the distribution of tsunami wave heights above the pre-tsunami sea level in Boundary Bay for Scenario-2 (1.0 m global sea level rise) and Scenario-3 (2.0 m global sea level rise). A major difference is that Scenario -3 will lead to significant flooding, which would occur in the western part of the bay, area D, and in the eastern part of the bay, in the river area A (see Figure 4 for the location). We note that the flooding would also overtop the updated dike.

Detailed distributions of tsunami heights for all three sea level scenarios are provided for specific areas: (A) Mud Bay (northeastern part of Boundary Bay; Figure 22); (B) The Semiahmoo area (Figure 23); (C) Drayton Harbor (Figure 24); and (D) Boundary Bay Park (Figure 25). The locations of the areas A, B, C, and D are shown in Figure 19.

The highest tsunami waves occur in Mud Bay (Figure 20). The increase in the initial sea level, by approximately 0.5 m between Scenarios 1 to 2, increases the tsunami amplitudes by 10% in Mud

Bay. A further increase in global sea level (Scenario-3) leads to an increase in the tsunami amplitude by 15%. In addition, for Scenario-3 a significant part of the area around the Nicomekl and Serpentine rivers will be flooded.

In the Semiahmoo region (Figure 23), an increase in global sea level will lead to a decrease in tsunami wave heights, but lead to flooding in the Campbell River valley and nearby low-lying areas. In both cases, the flooding is not related to the tsunami waves but to the initial sea level rise conditions.

In Drayton Harbor (Figure 24), the tsunami waves will reach an amplitude of about 1.1 – 1.3 m and will be nearly uniformly distributed over the harbour, excluding the harbour entrance. The tsunami amplitudes increase with the initial sea level increase for each scenario. For Scenario-3 (2.0 m rise in global sea level rise), Drayton Spit will be covered by water in several places.

Boundary Bay Park (Figure 25) will be completely underwater for Scenario-3, while for the other scenarios, the updated dike will protect the area from the tsunami waves. The tsunami amplitudes increase with increasing initial sea level for a givne scenario.

Detailed analyses of the sea level variability were carried out for 12 sites around Boundary Bay (Figures 26-28, Tables 3). The amplitudes and the shape of the tsunami records are similar for all scenarios and all sites. It is evident that the greatest difference is for the shallow sites (1-4), where the increase in sea level leads to a lowering of bottom friction and an accompanying prolongation of the tsunami oscillations.

Results of the water heights for the dike area are presented in Table 4. For Scenario-2 (global sea level rise of 1.0 m) and Scenario-3 (global sea level rise of 2.0 m), the “free board” in some places is less than the tsunami wave heights, indicating that the tsunami will overflow the areas.

3.2.2. Current speeds

Figure 29 shows the distribution of the tsunami-induced current maxima derived from the model for Scenario-1 (global sea level rise by 0.5 m) for 2 cases: (a) with the current dike configuration, and (b) with the increased dike height. As for the distribution of the tsunami heights (Figure 19), an increase in the dike height does not affect the distribution of the modelled current. In most places, the current will have moderate speeds of around 1 m/s (2 knots), except in specific areas,

where it could exceed 2 m/s. The rise in sea level will only weakly change the distribution of tsunami-induced currents (Figures 29-31).

In Mud Bay (Figure 32), the currents are strong (up to 3 m/s) in the southern part of the bay, along the rivers and in the Nicomekl River estuary. For Scenario-3 (Figure 32c), strong currents will flow over the dike as the tsunami spills over the dike into the adjoining low lands.

Currents along the Semiahmoo coast (area B, Figure 33) will generally be weak, except for at the mouth of Campbell River, where speeds could reach 2 m/s (4 knots). The current at the mouth of Campbell River will be stronger for Scenario-3 compared to Scenarios 1 and 2 because of the enhanced flooding in the river valley. The current at the entrance to Drayton Harbor (area C, Figure 34) will be strongest in the region and could reach 4 m/s (8 knots). Increasing sea level will decrease the current speed in the mouth of the harbour because of an increase in water depth. The maximum current at Boundary Bay Park (area D, Figure 35) will typically be below 1 m/s. The only exception is for Scenario S3 (global sea level rise of 2.0 m) when stronger (up to 2 m/s) currents will occur over the dike, when water overflows the dike at some points.

Details on the behaviour of the tsunami-induced currents for sites 1-12 are shown in Figures 36-41 and in Table 5. Generally, the current velocity time series are remarkably similar for all three sea level rise scenarios. The strongest currents (up to 1.35 m/s) are obtained at Site 8, located in the eastern sector of Boundary Bay. At other sites, modelled current speeds do not exceed 1 m/s.

The tsunami travel time to Boundary Bay from a CSZ earthquake is around 2:15-2:30 hours (first trough arrival time) and 2:40-3:10 hours (fist crest arrival time). The front crest wave is always highest and arrives first at sites 9,10, and 11, located on the Semiahmoo coast, then at sites 8 and 7 and, finally, at Site 1, approximately 25 min after hitting the Semiahmoo coast. The trailing waves are 2-3 times lower than the first wave.

In general, wave amplitudes associated with a CSZ tsunami are moderate in Boundary Bay and wave parameters change little with sea level rise. Sea level rise will increase the effect of tsunamis as tsunami flooding will be superposed on pre-tsunami sea levels. Tsunami-generated currents will not be significantly affected by sea level rise. However, the current is strong in narrow areas like the entrance to Drayton Harbor, where the wave-induced currents could be a hazard to small boats.

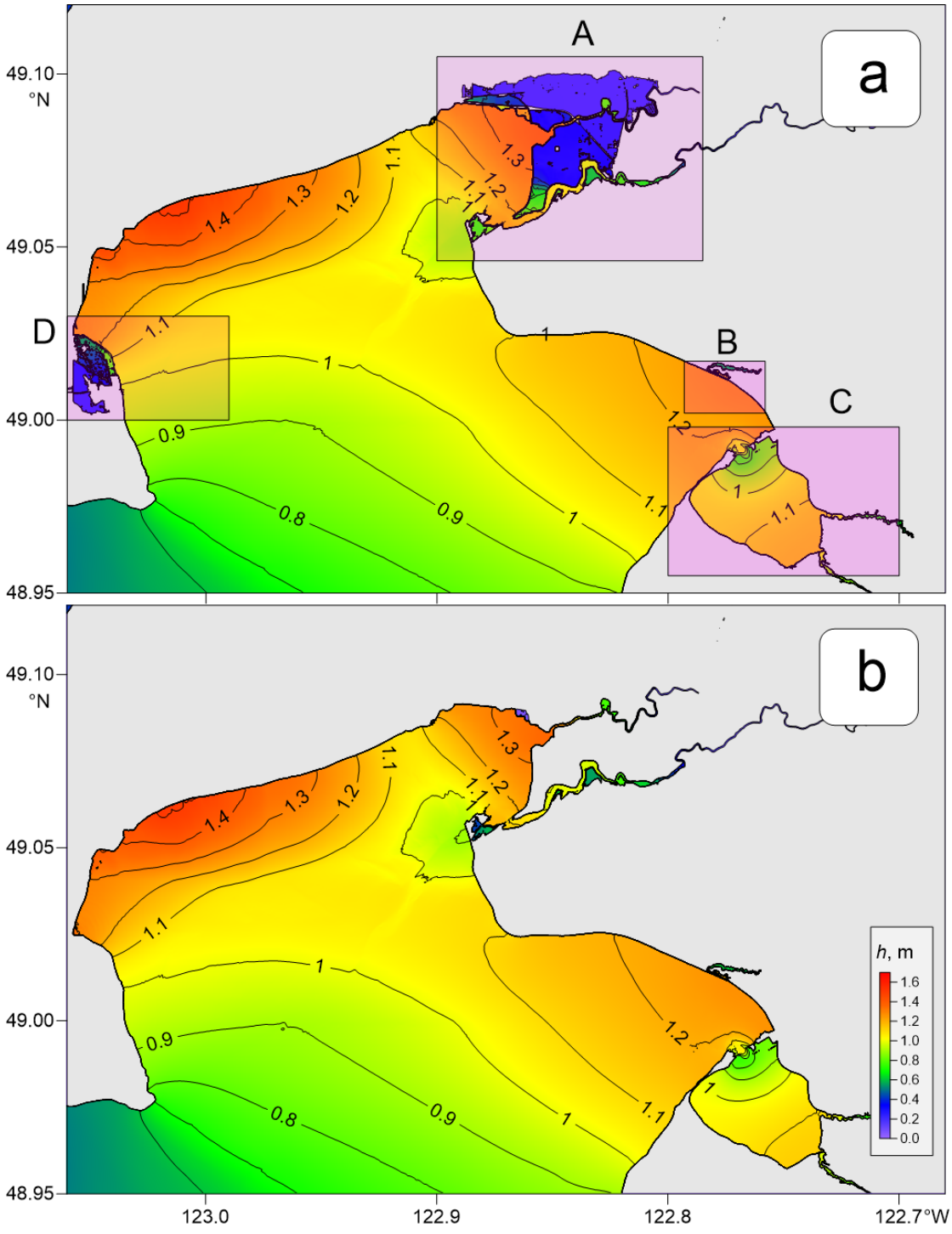

Figure 19. Distribution of maximum tsunami wave heights (*h*, metres) for Grid 4 of the nested-grid model for waves generated by simulation of the buried-type CSZ-type tsunami for the Scenario-1 future sea level rise condition (0.5 m global sea level rise) for: (a) the current dike configuration; and (b) for the updated dike with a height increase of 1.5 m.

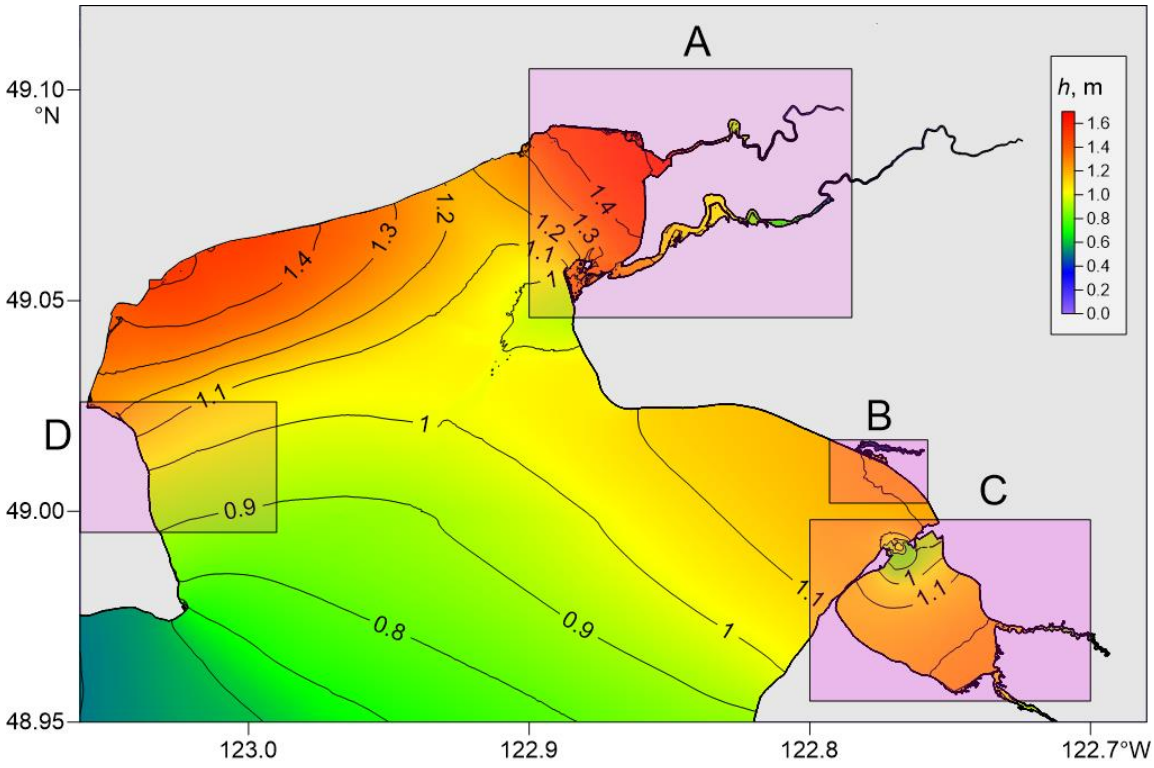

Figure 20. Distribution of maximum tsunami wave heights (*h*, metres) for Grid 4 of the nested-grid model for waves generated by simulation of the buried-type CSZ-type tsunami for the Scenario-2 future sea level rise condition (1.0 m global sea level rise) for the updated dike with height increased by 1.5 m.

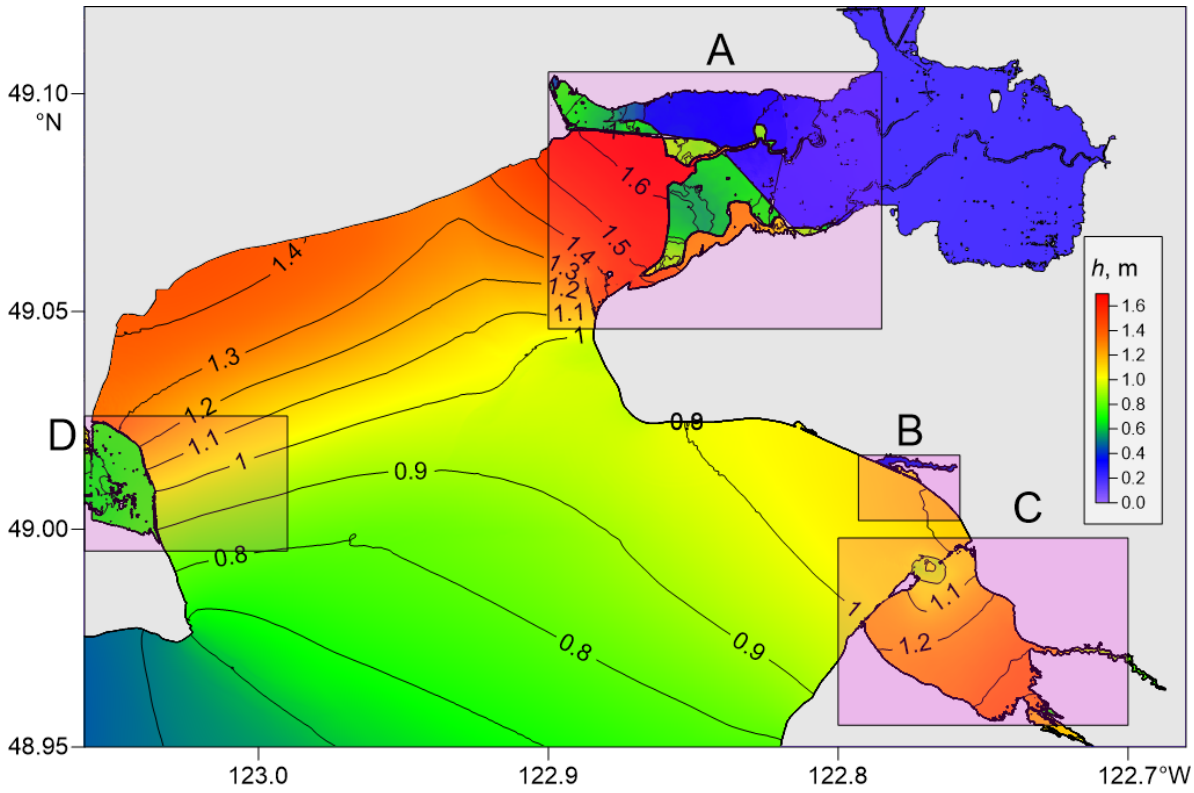

Figure 21. Distribution of maximum tsunami wave heights (*h*, metres) for Grid 4 of the nested-grid model for waves generated by simulation of the buried-type CSZ-type tsunami for the Scenario-3 future sea level rise condition (2.0 m global sea level rise) for an updated dike with height increased by 1.5 m.

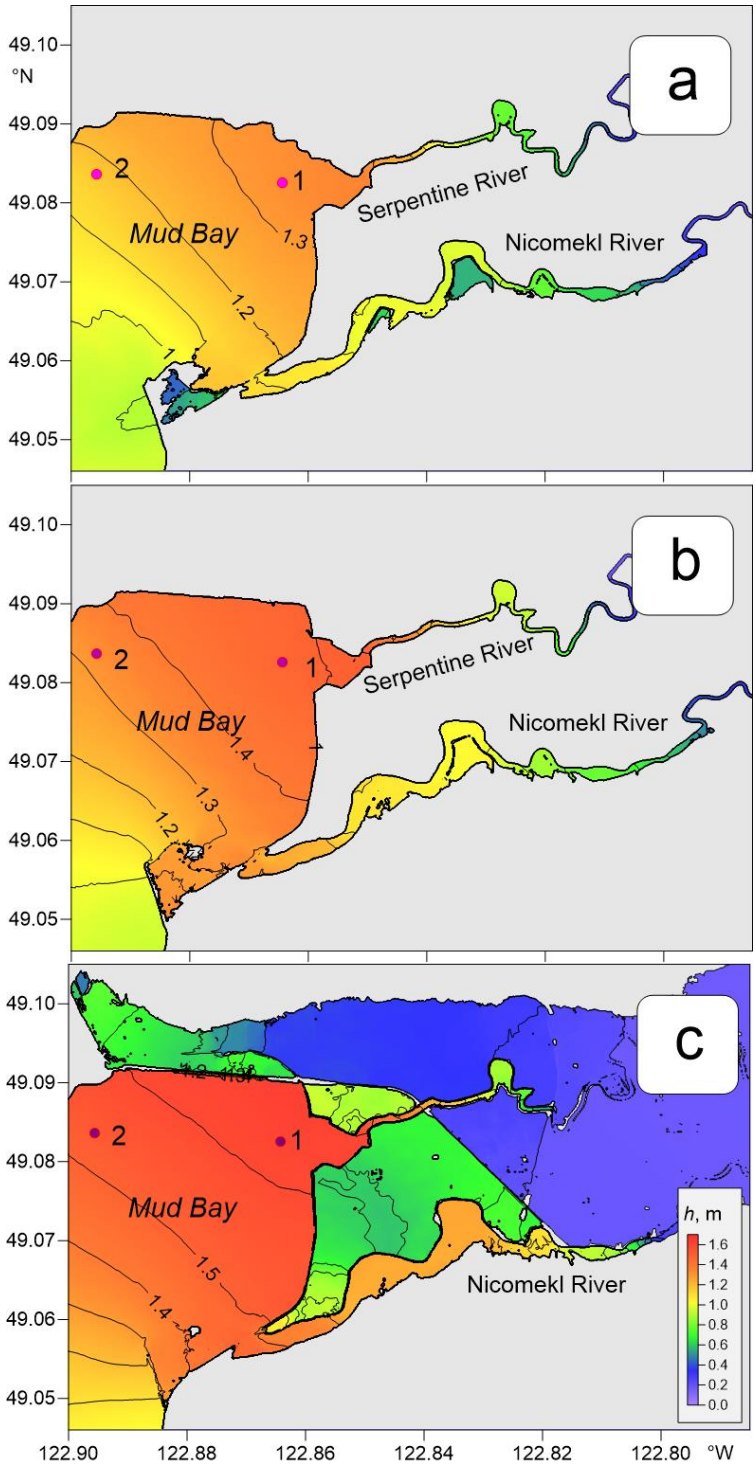

Figure 22. Distribution of maximum tsunami wave heights (*h*, metres) for region A (Mud Bay, see Figure 21 for the reference) for waves generated by simulation of the buried-type CSZ tsunami: (a) Scenario-1 (0.5 m global sea level rise case); (b) Scenario-2 (1 m global sea level rise case); and (c) Scenario-3 (2 m global sea level rise case). Numbers 1 and 2 denote sites for which tsunami wave records have been simulated.

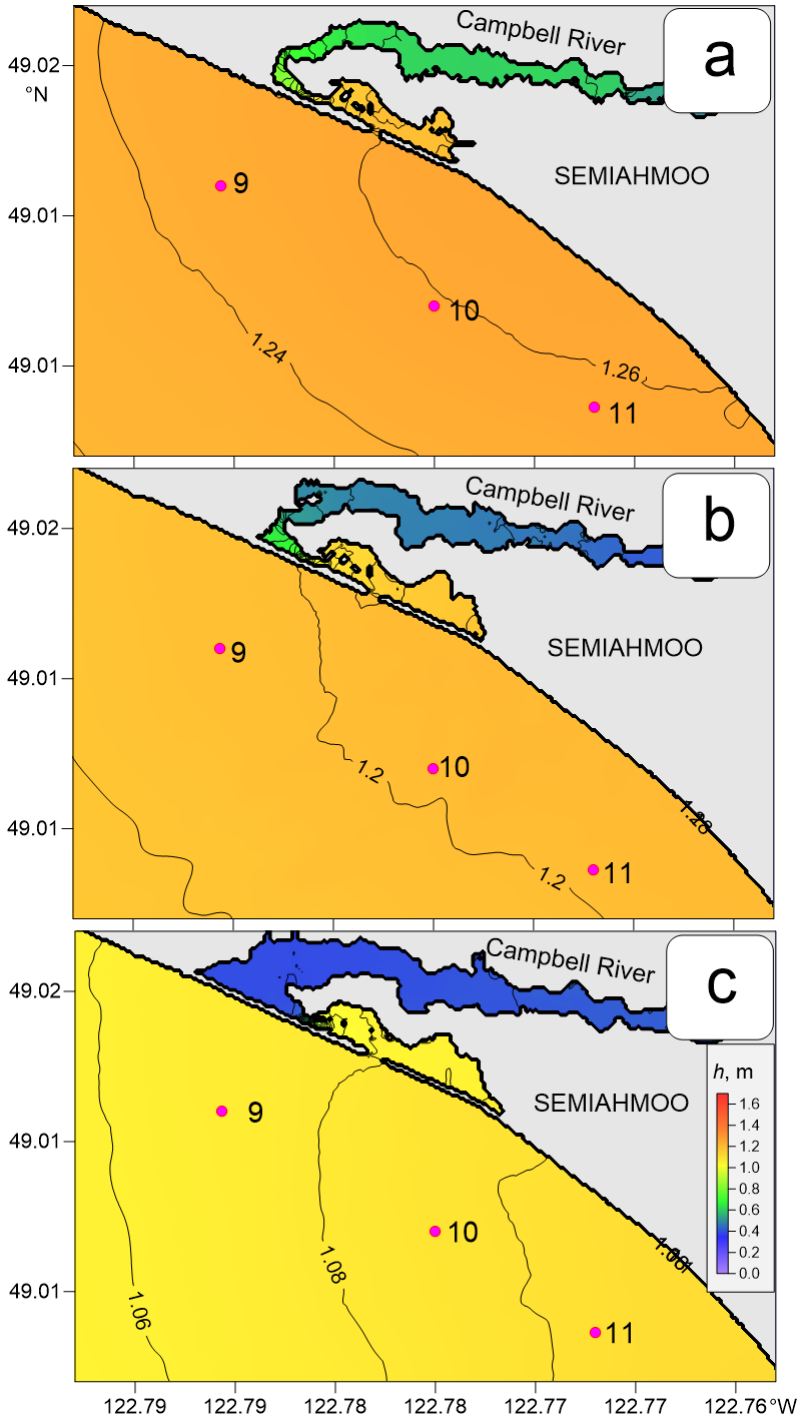

Figure 23. Distribution of maximum tsunami wave heights (*h*, metres) for Region B (Semiahmoo, see Figure 21 for the reference) for waves generated by simulation of the buried-type CSZ tsunami: (a) Scenario-1 (0.5 m global sea level rise case); (b) Scenario-2 (1 m global sea level rise case); and (c) Scenario-3 (2 m global sea level rise case). Numbers 9, 10, and 11 denote sites for which tsunami wave records have been simulated.

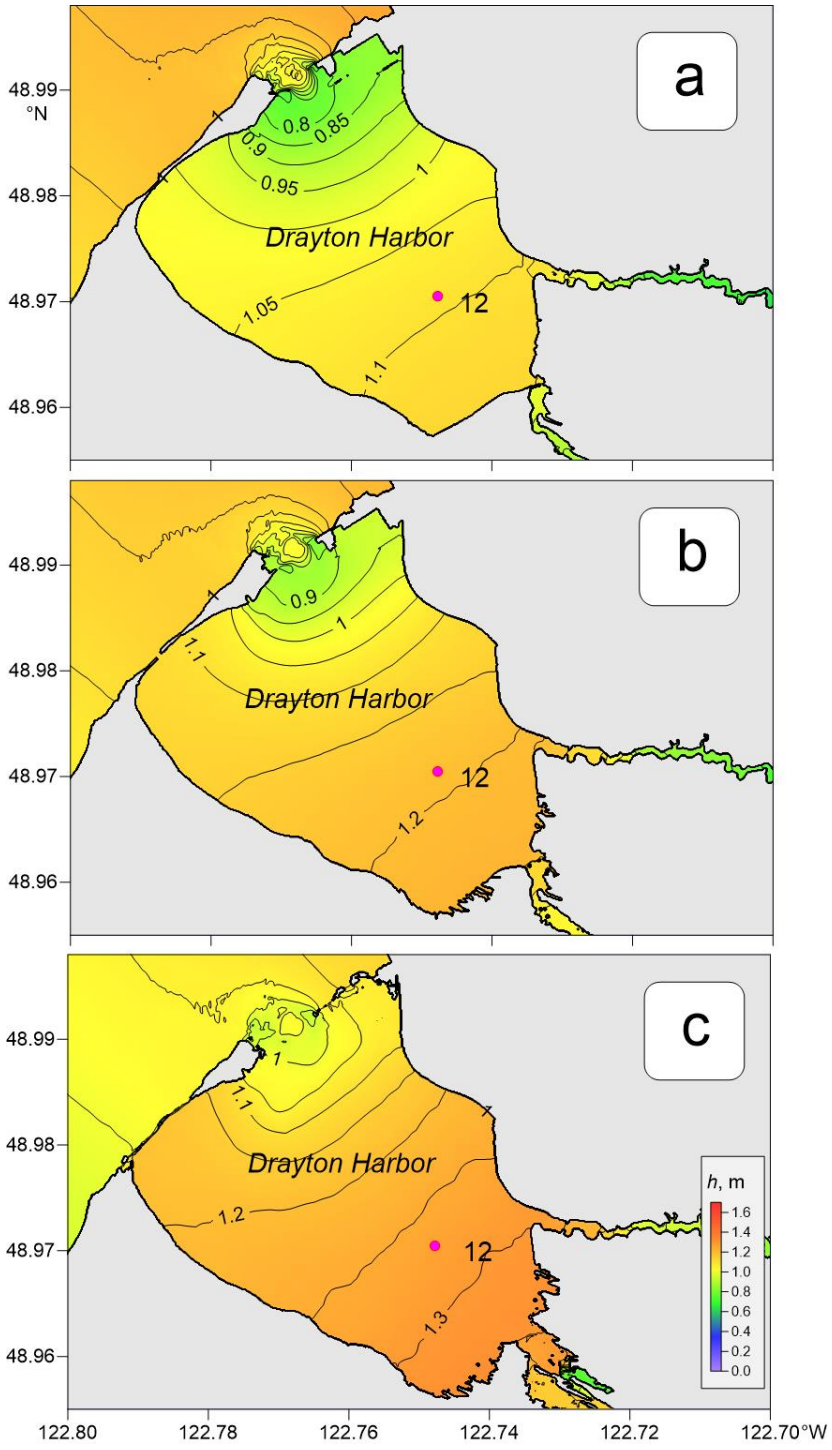

Figure 24. Distribution of maximum tsunami wave heights (*h*, metres) for Region C (Drayton Harbor, see Figure 21 for the reference) for waves generated by simulation of the buried-type CSZ tsunami: (a) Scenario-1 (0.5 m global sea level rise case); (b) Scenario-2 (1 m global sea level rise case); and (c) Scenario-3 (2 m global sea level rise case). Number 12 denotes site for which tsunami wave records have been simulated.

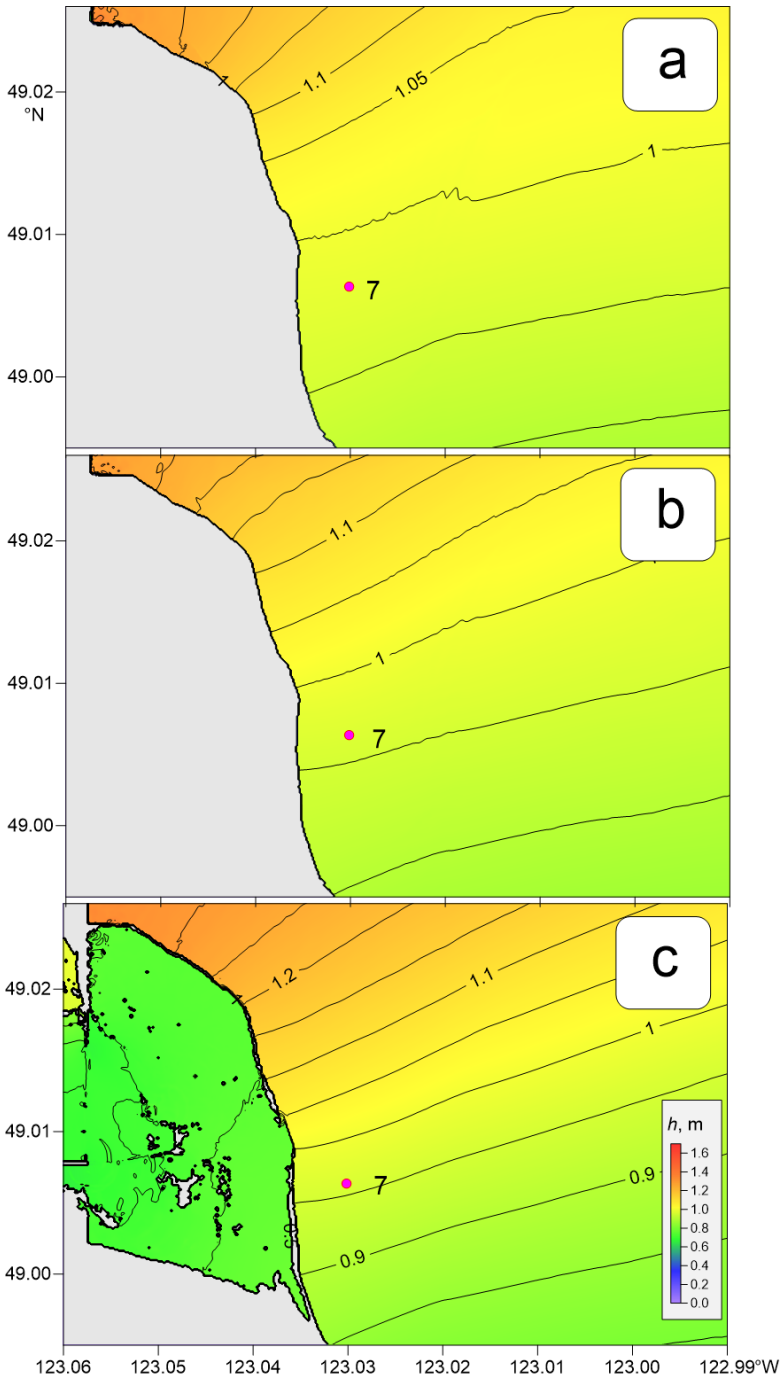

Figure 25. Distribution of maximum tsunami wave heights (*h*, metres) for Region D (Boundary Bay Park; see Figure 21 for) for waves generated by simulation of the buried-type CSZ tsunami for scenarios S1 (a), S2 (b), and S3 (c). Number 7 denotes site for which tsunami wave records have been simulated.

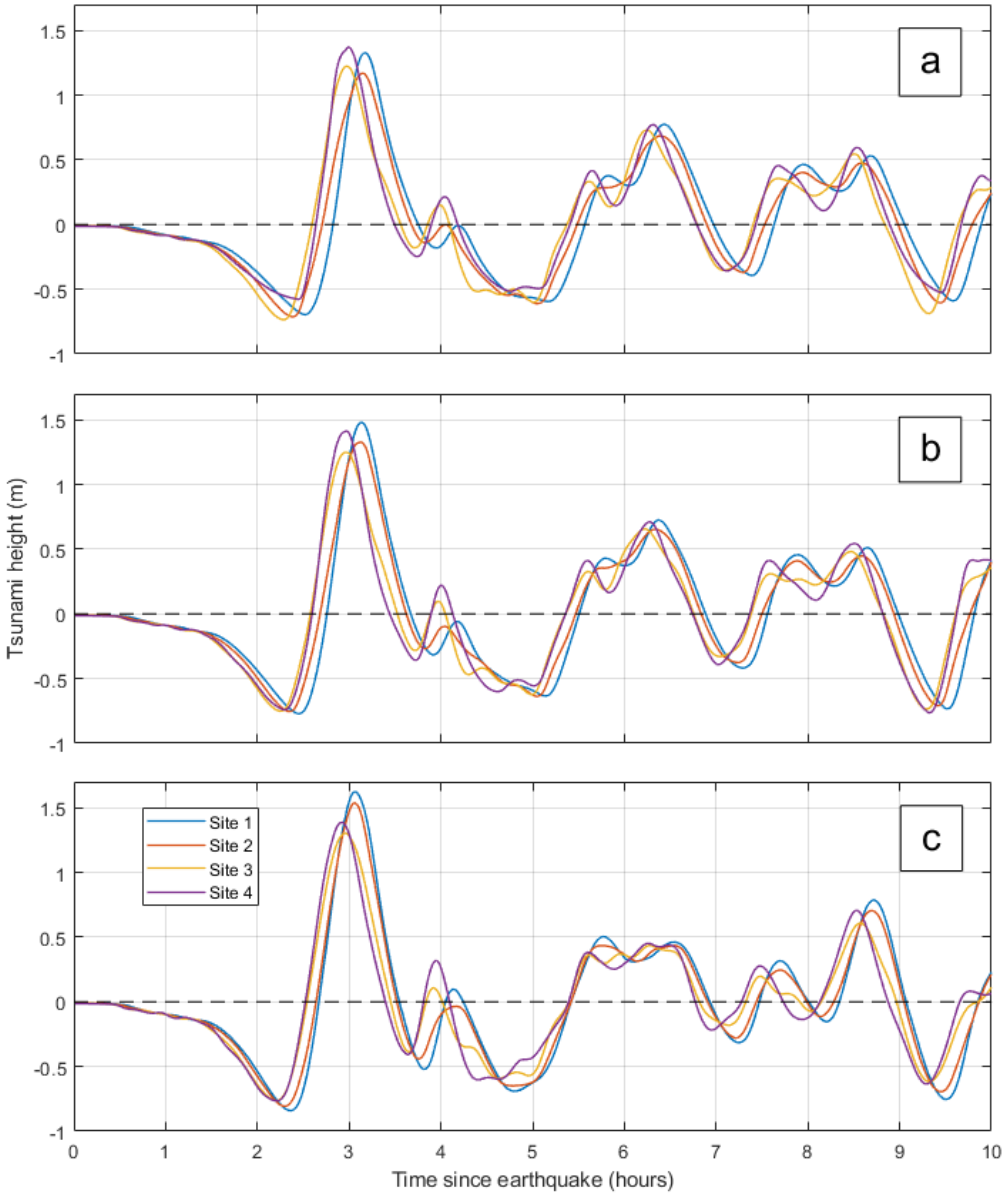

Figure 26. Simulated records of sea level variation for the CSZ tsunami at sites 1 – 4 for sea level rise: (a) Scenario-1 (0.5 m global sea level rise case); (b) Scenario-2 (1 m global sea level rise case); and (c) Scenario-3 (2 m global sea level rise case). See Figure 4 for the site locations.

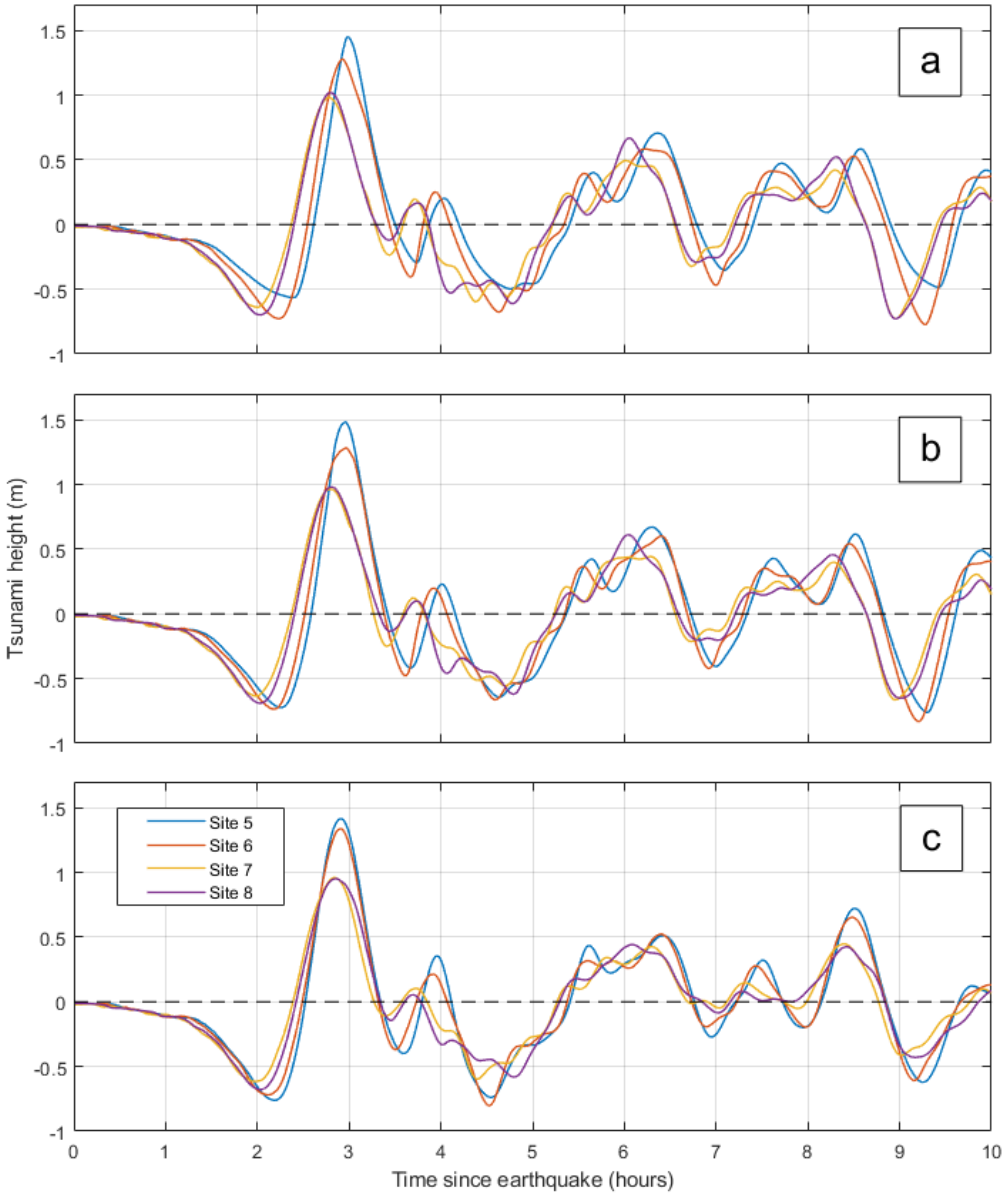

Figure 27. Simulated records of sea level variation for the CSZ tsunami at sites 5 – 8 for sea level rise: (a) Scenario-1 (0.5 m global sea level rise case); (b) Scenario-2 (1 m global sea level rise case); and (c) Scenario-3 (2 m global sea level rise case). See Figure 4 for the site locations.

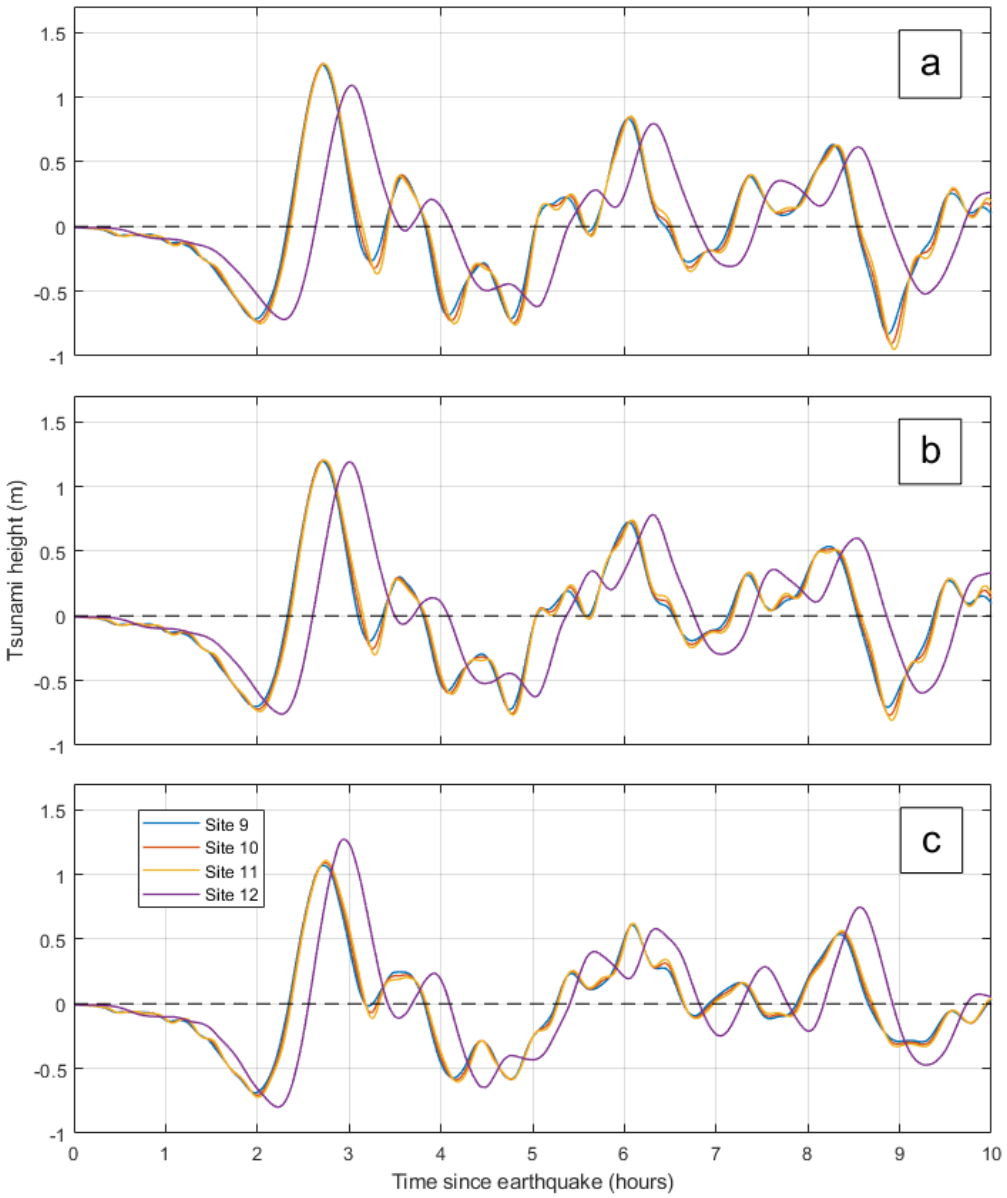

Figure 28. Simulated records of sea level variation for the CSZ tsunami at sites 9 – 12 (a): Scenario-1 (0.5 m global sea level rise case); (b) Scenario-2 (1 m global sea level rise case); and (c) Scenario-3 (2 m global sea level rise case). See Figure 4 for the site locations.

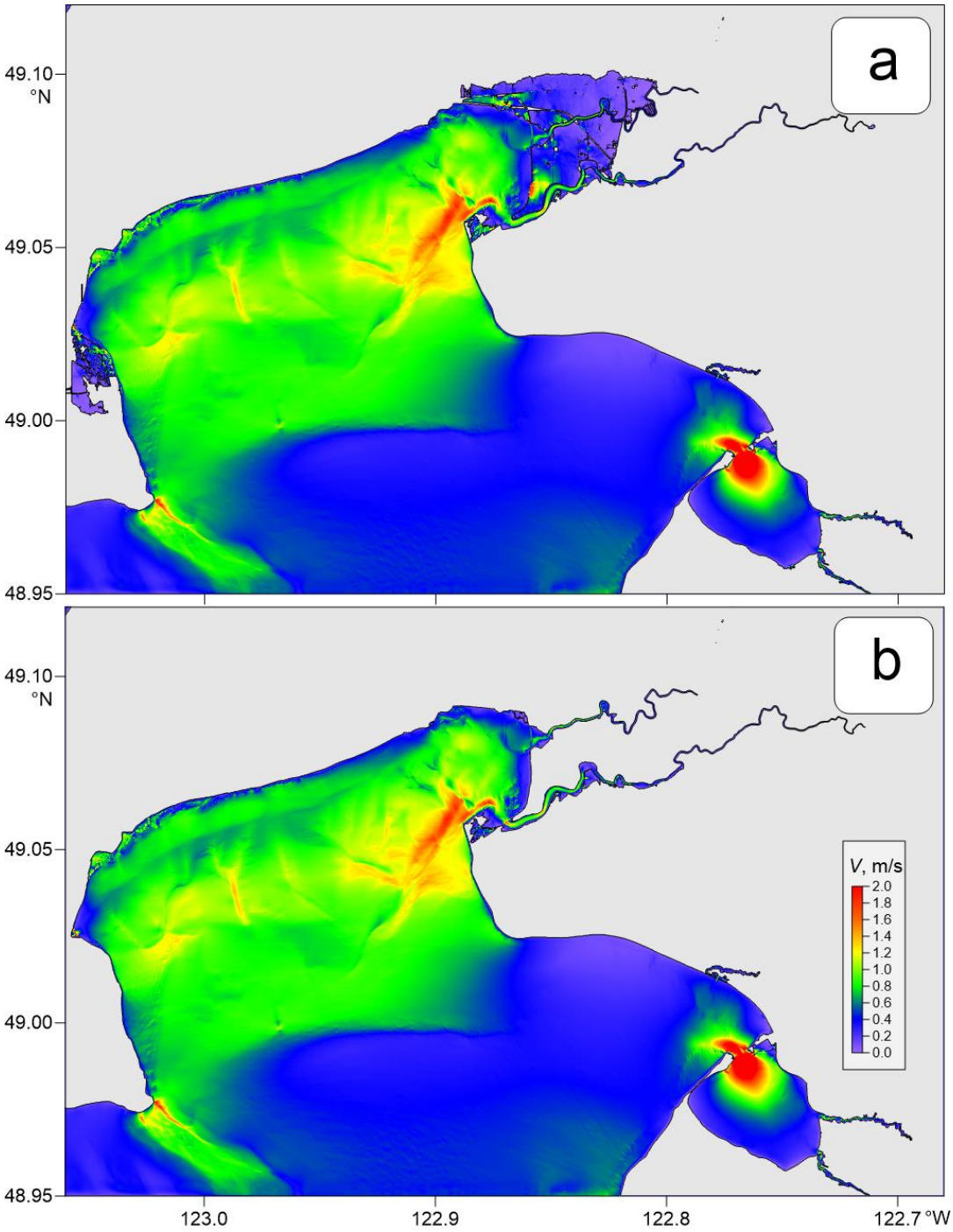

Figure 29. Distribution of maximum tsunami generated current (*V*, m/s) for Grid 4 of the nested-grid model for waves generated by simulation of the CSZ tsunami for the Scenario-1 future sea level rise condition (0.5 m global sea level rise) for (a) current dike, and (b) updated dike with increased height by 1.5 m.

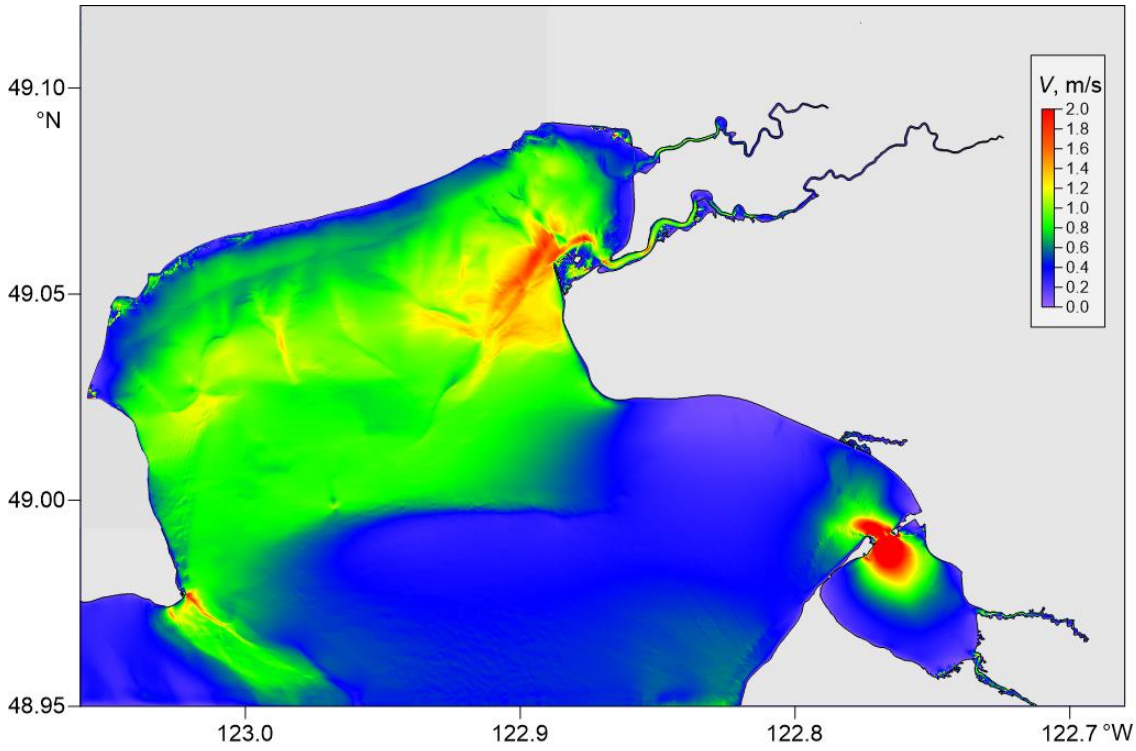

Figure 30. Distribution of maximum tsunami generated current (V, m/s) for Grid 4 of the nested-grid model for waves generated by simulation of the buried-type CSZ tsunami for the Scenario-2 future sea level rise condition (1.0 m global sea level rise).

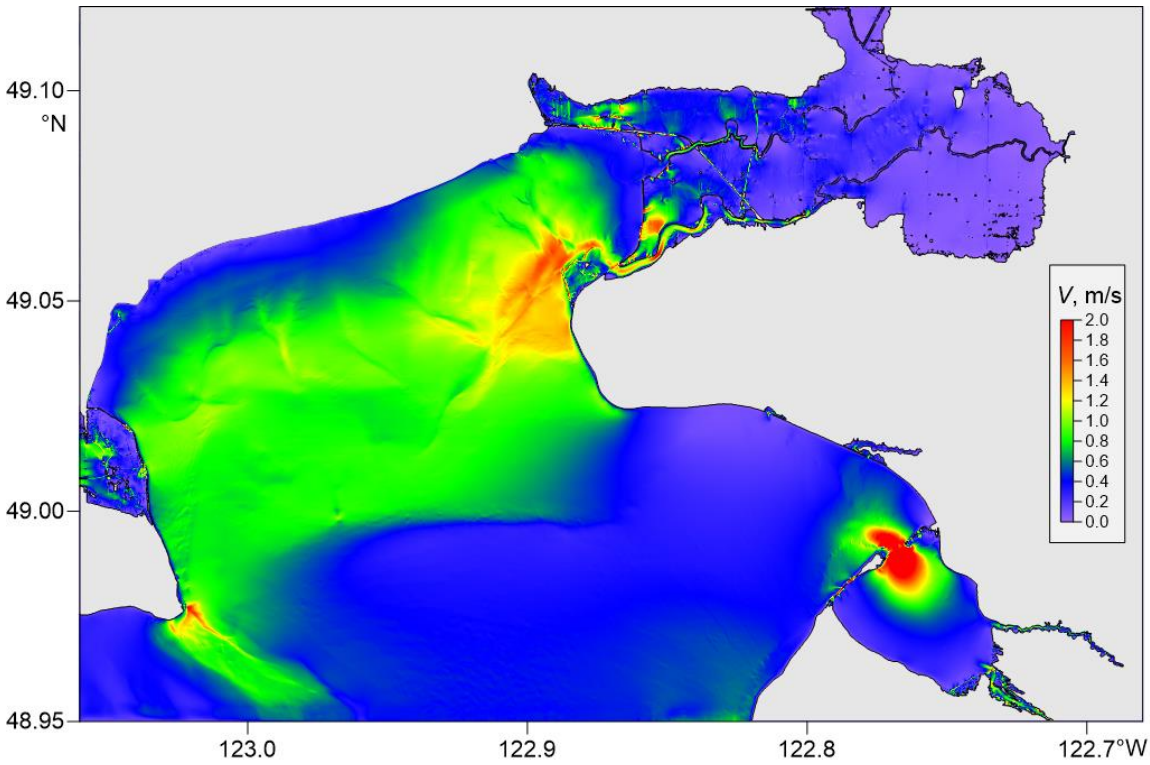

Figure 31. Distribution of maximum tsunami generated current (*V*, m/s) for Grid 4 of the nested-grid model for waves generated by simulation of the buried-type CSZ tsunami for the Scenario-3 future sea level rise condition (2.0 m global sea level rise).

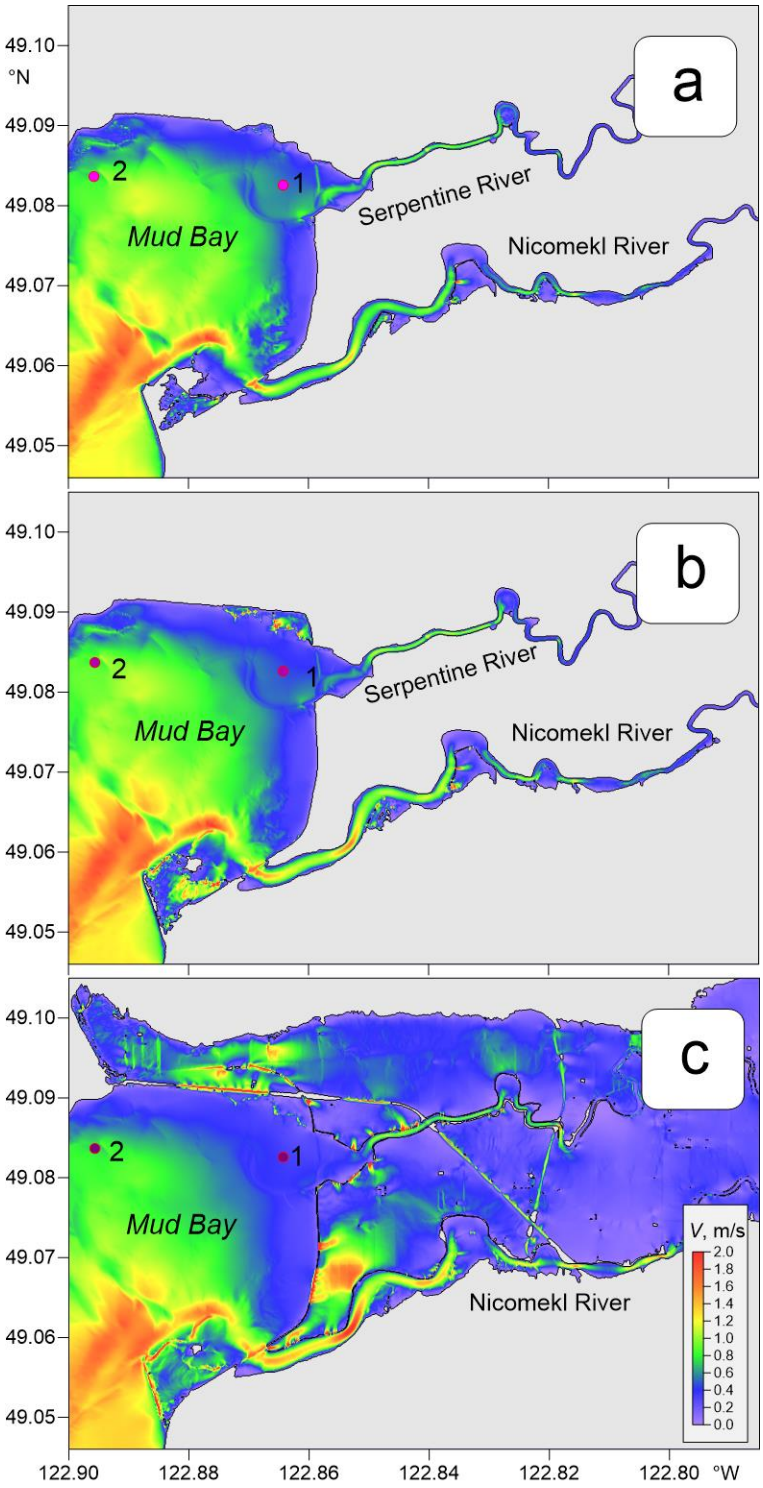

Figure 32. Distribution of maximum tsunami generated currents (V, m/s) for Region A (Mud Bay, see Figure 21 for the reference) for waves generated by simulation of the buried-type CSZ tsunami: (a) Scenario-1 (0.5 m global sea level rise case); (b) Scenario-2 (1 m global sea level rise case); and (c) Scenario-3 (2 m global sea level rise case).

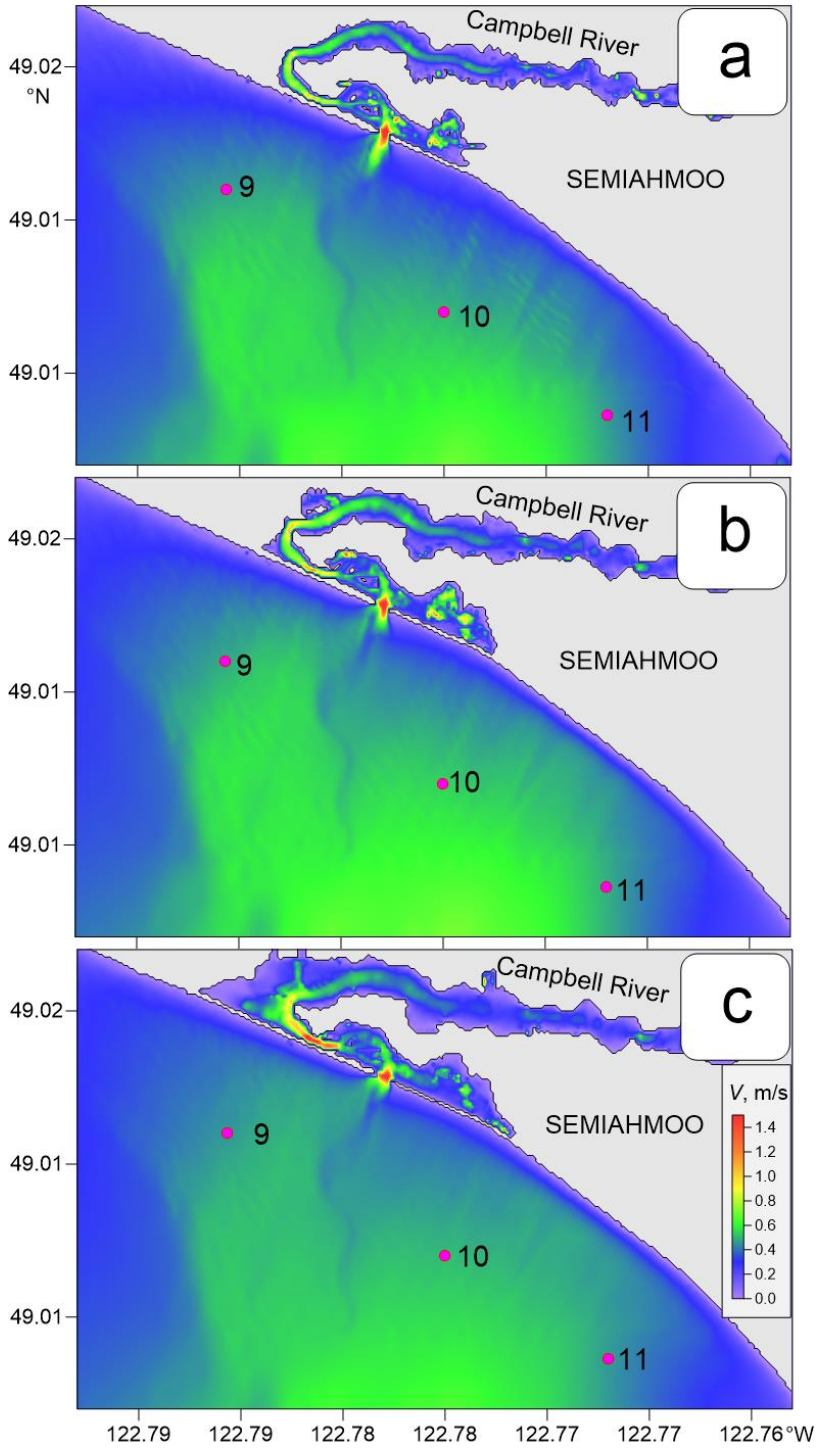

Figure 33. Distribution of maximum tsunami generated currents (*V*, m/s) for Region B (Semiahmoo, see Figure 21 for the reference) for waves generated by simulation of the buried-type CSZ tsunami: (a) Scenario-1 (0.5 m global sea level rise case); (b) Scenario-2 (1 m global sea level rise case); and (c) Scenario-3 (2 m global sea level rise case).

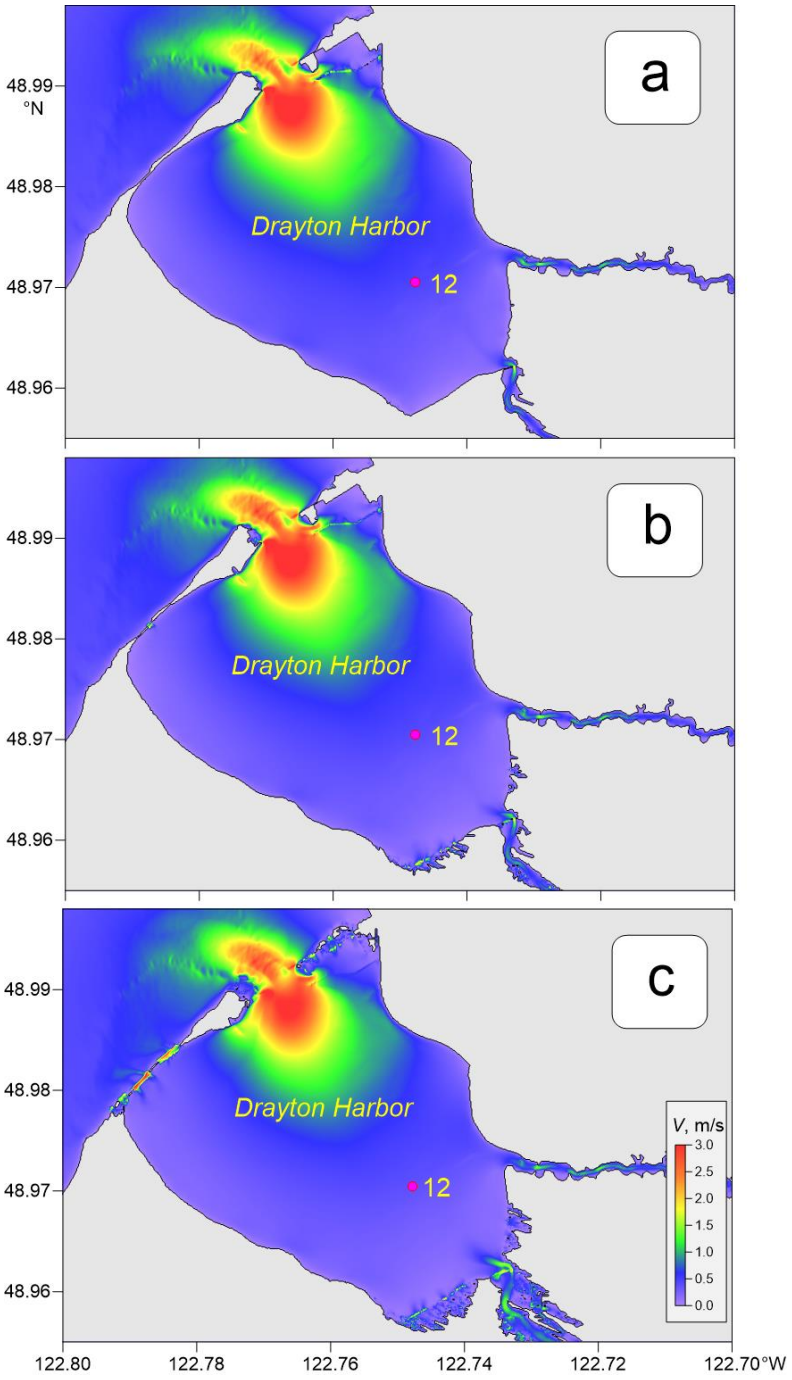

Figure 34. Distribution of maximum tsunami generated currents (*V*, m/s) for Region C (Dayton Harbor, see Figure 21) for waves generated by simulation of the buried-type CSZ tsunami: (a) Scenario-1 (0.5 m global sea level rise case); (b) Scenario-2 (1 m global sea level rise case); and (c) Scenario-3 (2 m global sea level rise case).

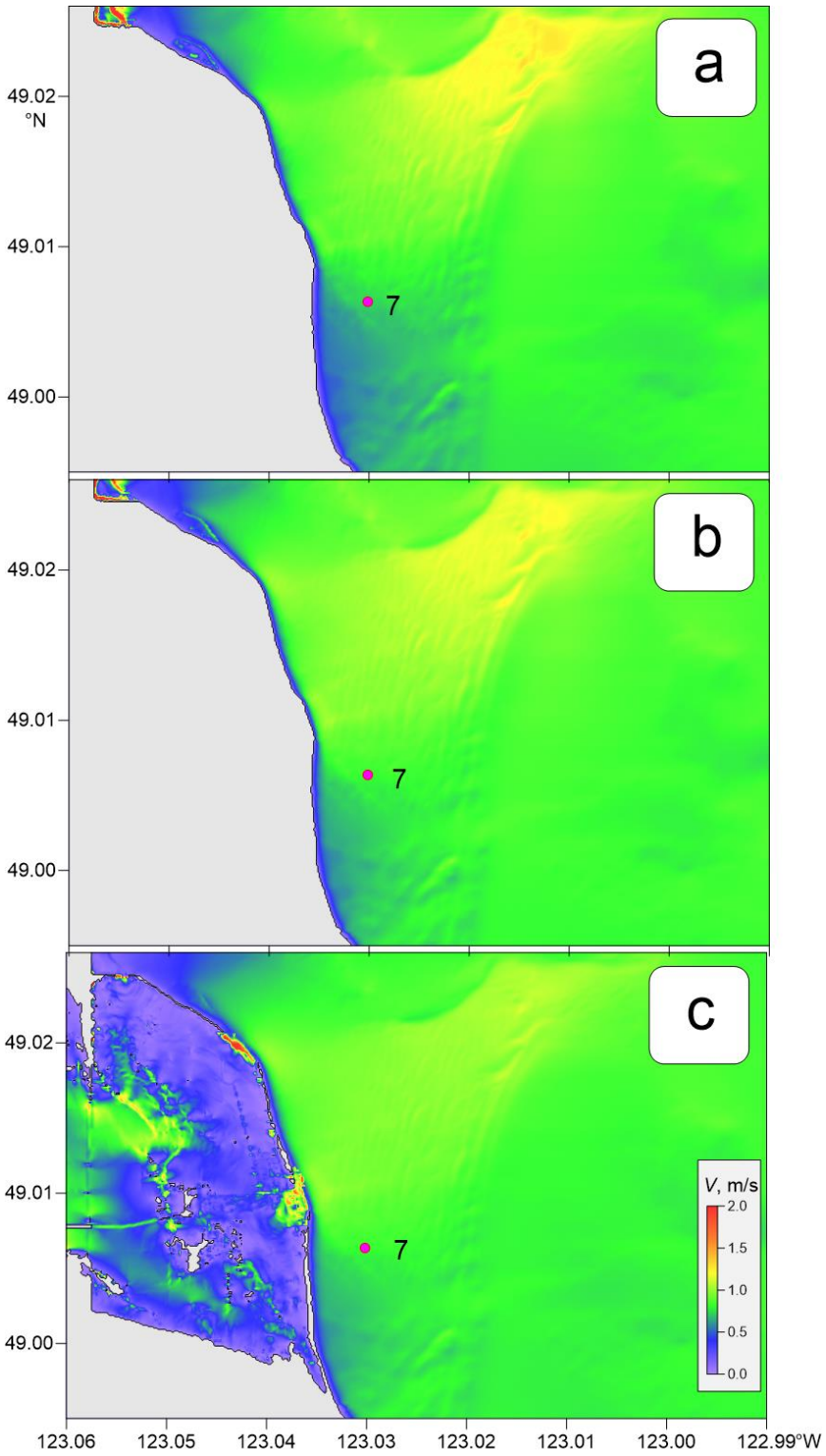

Figure 35. Distribution of maximum tsunami generated currents (V, m/s) for Region D (Boundary Bay Park; see Figure 21) for waves generated by simulation of the buried-type CSZ tsunami: (a) Scenario-1 (0.5 m global sea level rise case); (b) Scenario-2 (1 m global sea level rise case); and (c) Scenario-3 (2 m global sea level rise case).

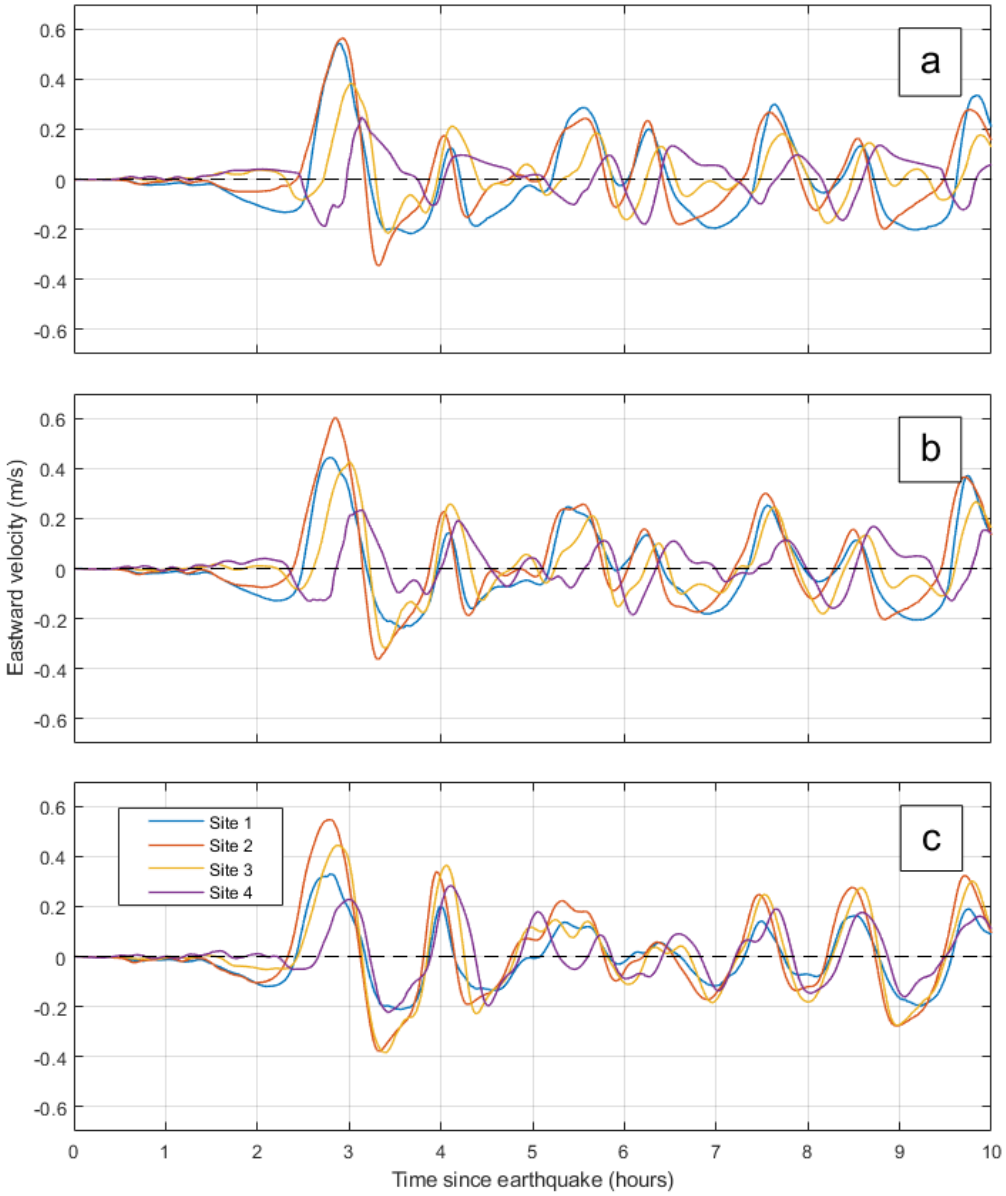

Figure 36. Simulated records of the eastward component of current velocity, *V*, for the CSZ tsunami at sites 1-4: (a) Scenario-1 (0.5 m global sea level rise case); (b) Scenario-2 (1 m global sea level rise case); and (c) Scenario-3 (2 m global sea level rise case). See Figure 4 for the site locations.

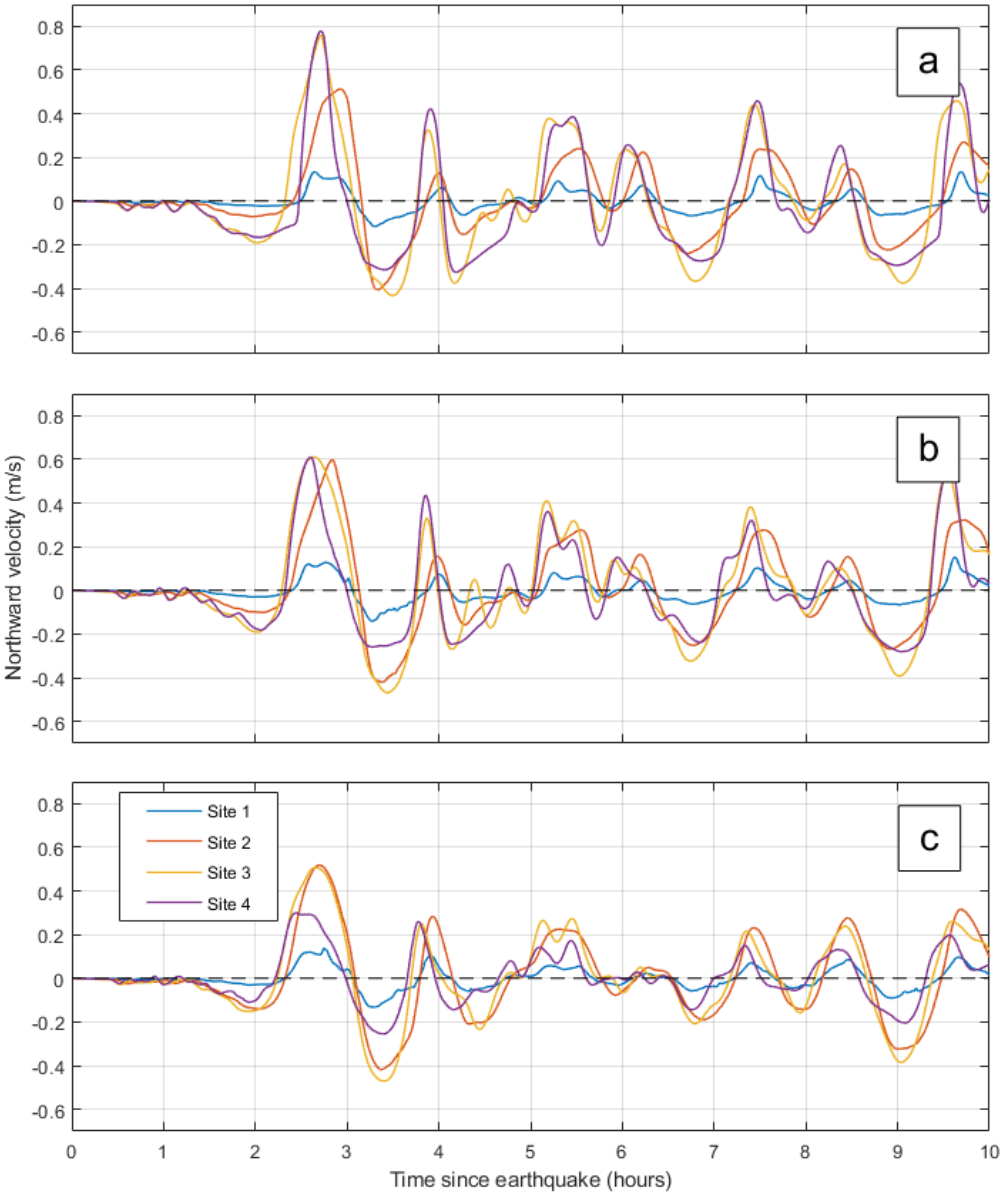

Figure 37. Simulated records of the northward component of current velocity for the CSZ tsunami at sites 1-4: (a) Scenario-1 (0.5 m global sea level rise case); (b) Scenario-2 (1 m global sea level rise case); and (c) Scenario-3 (2 m global sea level rise case). See Figure 4 for the site locations.

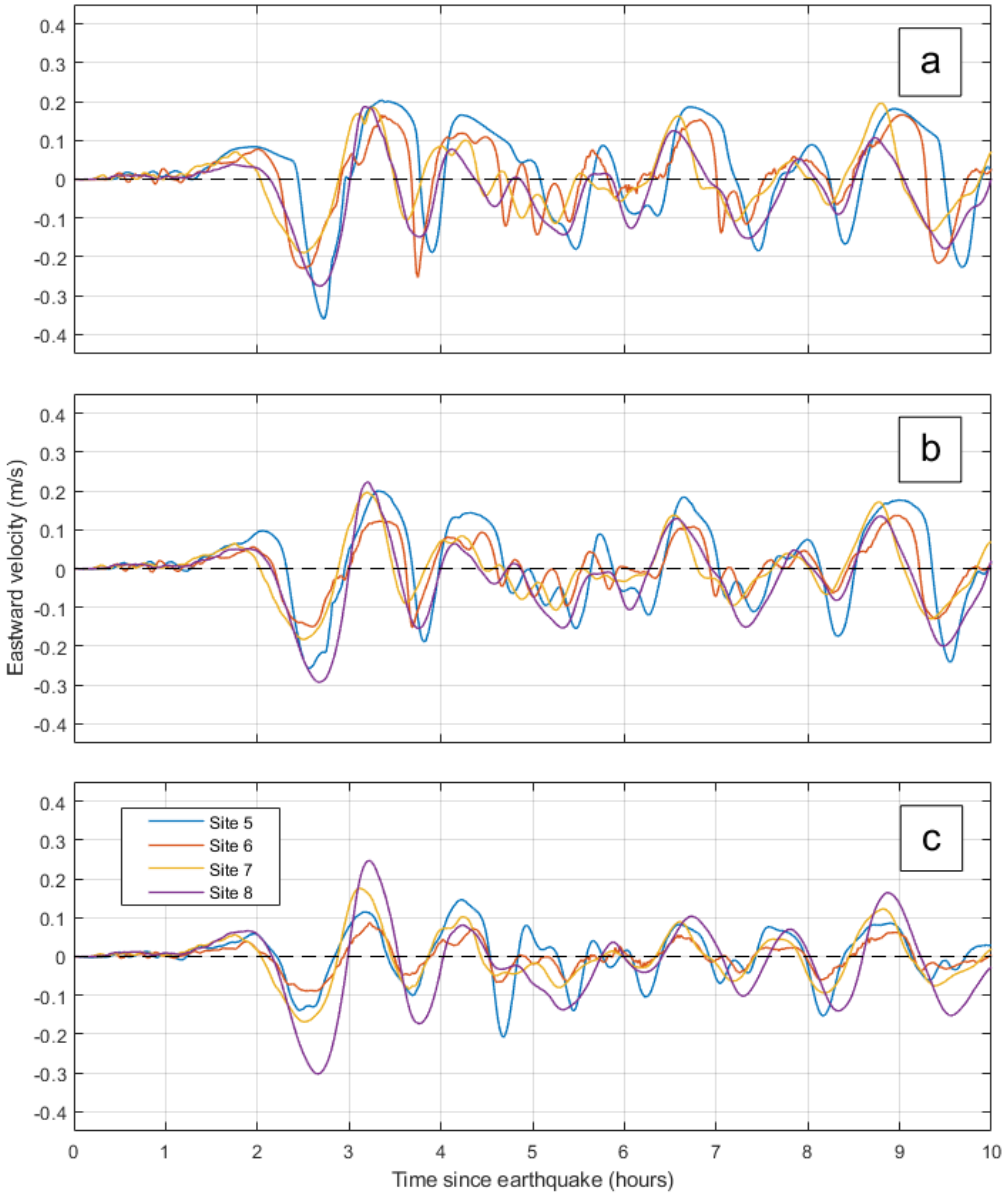

Figure 38. Simulated records of the eastward component of current velocity for the CSZ tsunami at sites 5-8: (a) Scenario-1 (0.5 m global sea level rise case); (b) Scenario-2 (1 m global sea level rise case); and (c) Scenario-3 (2 m global sea level rise case). See Figure 4 for the site locations.

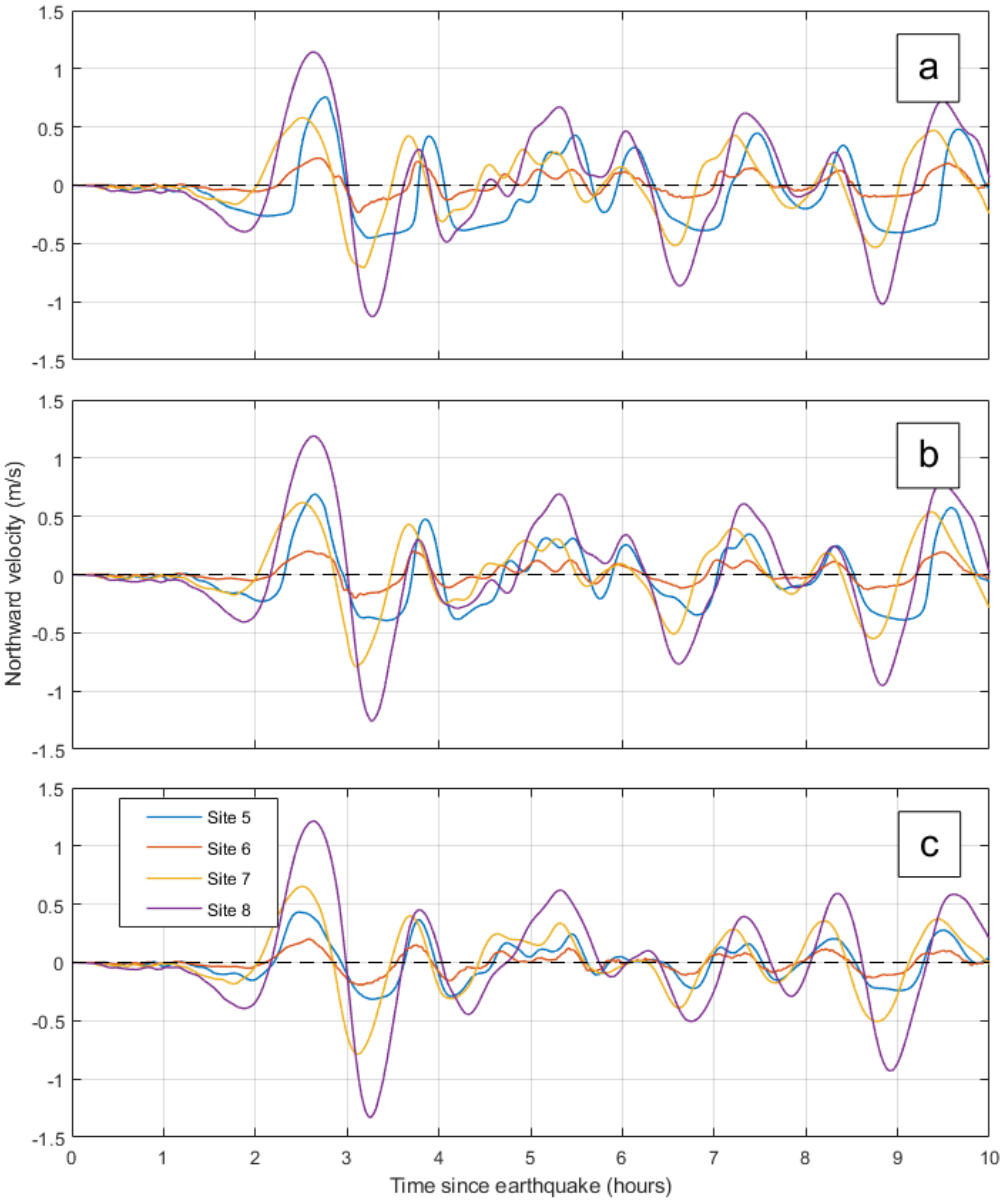

Figure 39. Simulated records of the northward component of current velocity for the CSZ tsunami at sites 5-8: (a) Scenario-1 (0.5 m global sea level rise case); (b) Scenario-2 (1 m global sea level rise case); and (c) Scenario-3 (2 m global sea level rise case). See Figure 4 for the site locations.

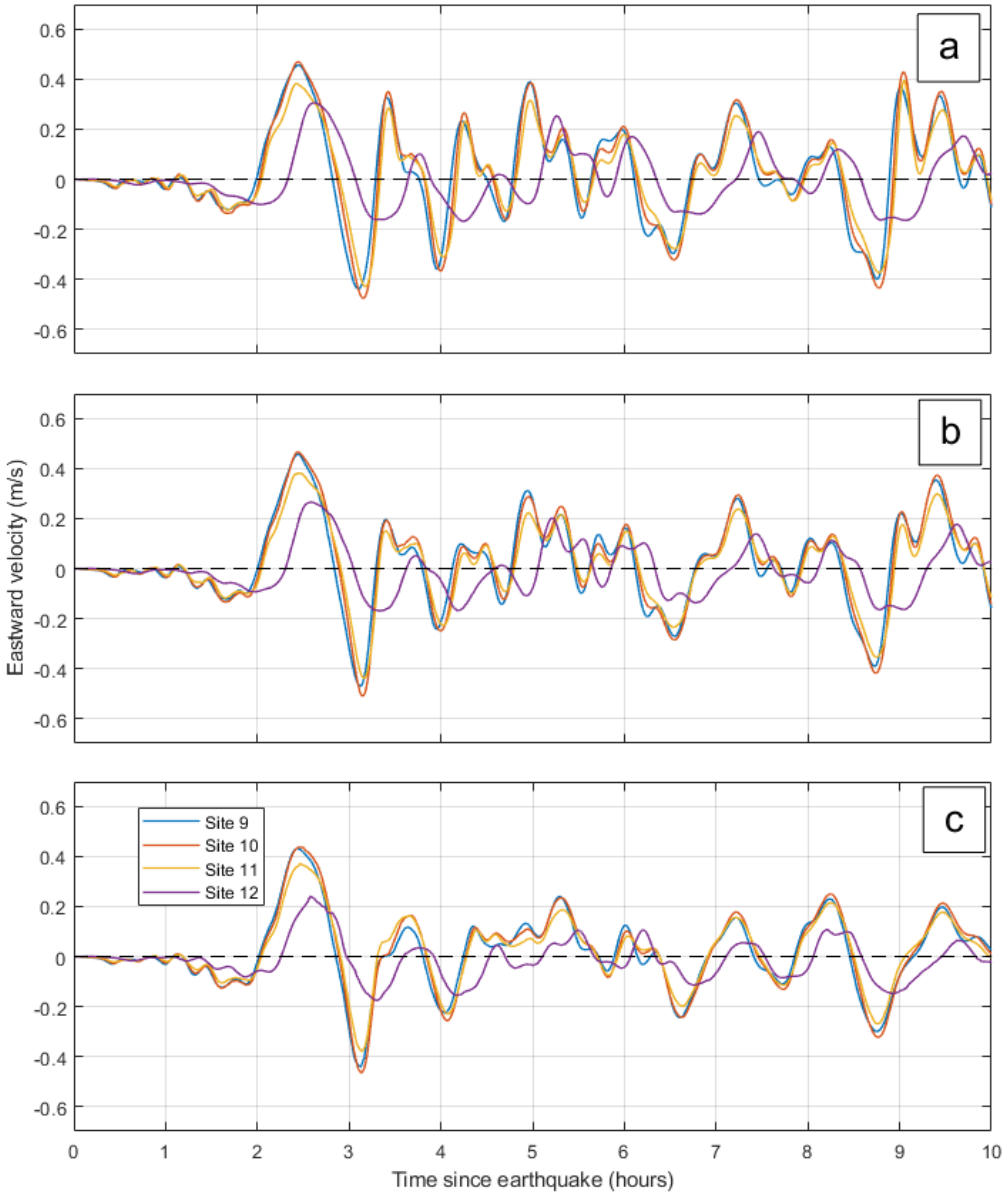

Figure 40. Simulated records of the eastward component of current velocity for the CSZ tsunami at sites 9-12: (a) Scenario-1 (0.5 m global sea level rise case); (b) Scenario-2 (1 m global sea level rise case); and (c) Scenario-3 (2 m global sea level rise case). See Figure 4 for the site locations.

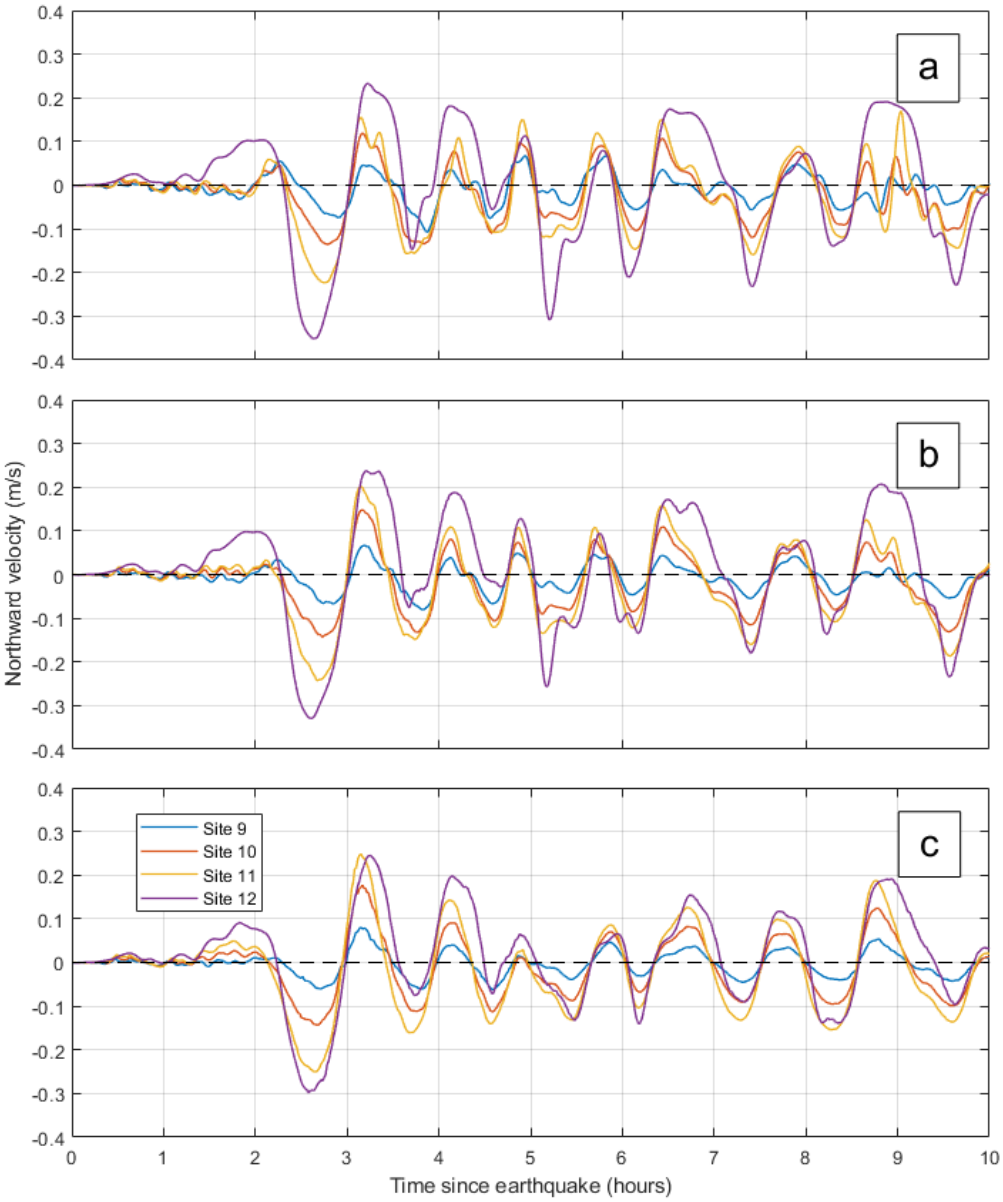

Figure 41. Simulated records of the northward component of current velocity for the CSZ tsunami at sites 9-12: (a) Scenario-1 (0.5 m global sea level rise case); (b) Scenario-2 (1 m global sea level rise case); and (c) Scenario-3 (2 m global sea level rise case). See Figure 4 for the site locations.

Table 3. Tsunami wave parameters for the CSZ buried-fault earthquake and tsunami at Boundary Bay for numerical simulations for the three sea level rise scenarios, S1 to S3. See Figure 4 for the site locations. Travel times for the maximum waves are in hours and minutes (hh:mm) after the start of the earthquake.

Site No	Highest crest						Deepest trough					
	Height (m)			Travel time (hh:mm)			Height (m)			Travel time (hh:mm)		
	S1	S2	S3	S1	S2	S3	S1	S2	S3	S1	S2	S3
1	1.33	1.48	1.62	3:10	3:08	3:04	-0.70	-0.77	-0.84	2:31	2:27	2:22
2	1.17	1.33	1.54	3:09	3:08	3:04	-0.71	-0.75	-0.81	2:23	2:21	2:18
3	1.22	1.25	1.30	2:58	2:58	2:58	-0.74	-0.75	-0.77	2:17	2:15	2:12
4	1.37	1.41	1.39	2:60	2:59	2:55	-0.58	-0.76	-0.77	2:27	9:20	2:13
5	1.45	1.48	1.41	2:59	2:57	2:55	-0.57	-0.76	-0.76	2:23	9:18	2:11
6	1.28	1.28	1.34	2:56	2:58	2:54	-0.77	-0.83	-0.80	9:17	9:12	4:32
7	0.98	0.96	0.96	2:47	2:48	2:50	-0.73	-0.66	-0.62	8:57	8:57	1:58
8	1.02	0.98	0.95	2:48	2:48	2:51	-0.73	-0.69	-0.68	8:57	2:02	2:02
9	1.25	1.19	1.07	2:43	2:42	2:43	-0.83	-0.72	-0.69	8:52	4:45	1:59
10	1.26	1.20	1.09	2:43	2:43	2:44	-0.90	-0.77	-0.71	8:55	8:54	1:60
11	1.26	1.20	1.11	2:44	2:44	2:45	-0.95	-0.81	-0.72	8:56	8:55	1:60
12	1.09	1.19	1.27	3:02	2:60	2:57	-0.72	-0.76	-0.80	2:18	2:16	2:13

Table 4. Heights of the present-day Dike and Higher High Water Mean Tide (HHWMT) along the shores of Boundary Bay for the cross-sections shown in Figure 9. "Free-board" = Height of Dike – HHWMT is the difference in elevation between the dike and the average Higher High Water level (HHW) during a year (in sailing terms, "free-board" is how high above the waterline is the water before the desks become awash). S1 to S3 denote the three sea level rise Scenarios.

Section	Height of Dike (m)	Height of HHWMT (m)			Free-board (m)			Maximum wave height (m)		
		S1	S2	S3	S1	S2	S3	S1	S2	S3
A1	3.11	1.71	2.16	3.06	1.40	0.95	0.05	1.27	1.25	1.31
A2	3.42	1.71	2.16	3.06	1.71	1.26	0.36	1.28	1.28	1.34
B1	3.74	1.71	2.17	3.07	2.03	1.57	0.67	1.41	1.46	1.40
B2	3.68	1.71	2.17	3.07	1.97	1.50	0.59	1.23	1.25	1.31
C1	4.75	1.72	2.17	3.08	3.03	2.60	1.67	1.31	1.47	1.60
C2	2.75	1.72	2.17	3.08	1.03	0.60	-0.33	1.25	1.41	1.55

Comments:

Higher High Water Large Tide (HHWLT), the average highest water in a year, is 0.66 m higher than HHWMT for Pt. Atkinson and Vancouver.

The highest observed water level for Pt. Atkinson is 1.22 m above HHWMT, and for Vancouver 1.26 m above HHWMT.

Table 5. Wave-induced current speeds (V) for the numerical simulations of the buried-fault CSZ-type tsunami in Boundary Bay for the three sea level rise scenarios S1-S3. See Figure 4 for the site locations. The times for the occurrence of maximum wave-induced currents are in hours and minutes (hh:mm) after the start of the earthquake.

	Maximum current speed (m/s)			Travel time to maximum current (hh:mm)		
	S1	S2	S3	S1	S2	S3
1	0.55	0.46	0.35	2:54	2:48	2:47
2	0.76	0.85	0.75	2:56	2:51	2:44
3	0.76	0.61	0.62	2:43	2:39	2:47
4	0.80	0.62	0.34	2:43	2:36	3:25
5	0.83	0.73	0.45	2:44	2:39	2:28
6	0.32	0.25	0.22	3:45	2:35	2:35
7	0.72	0.81	0.81	3:11	3:06	3:07
8	1.18	1.27	1.35	2:38	3:16	3:15
9	0.46	0.47	0.45	2:27	3:07	3:07
10	0.49	0.53	0.50	3:09	3:09	3:08
11	0.45	0.48	0.45	3:10	3:10	3:08
12	0.46	0.42	0.38	2:38	2:36	2:35

4. CONCLUSIONS

A high-resolution, nested-grid tsunami model has been used to simulate the distribution of tsunami waves and wave-induced currents that will be generated in Boundary Bay during a buried-rupture Cascadia Subduction Zone (CSZ), momentum magnitude M_w 9.0 earthquake for three future sea level rise scenarios: S1, a 0.5 m global sea level rise scenario, corresponding to the median RCP8.5 model; S2, a 1.0 m global sea level rise scenario, corresponding to the upper RCP8.5 climate model; and S3, a 2.0 m global sea level rise, referred as the year 2200 model. The tsunami model uses an advanced tsunami source distribution and high-resolution bathymetry for the area of interest. The major results of the modelling are:

- The initial model conditions for scenarios S2 and S3 required an increase in the height of the dike situated along the northern coast of Boundary Bay and along the Serpentine and Nicomekl rivers. Without an increase in dike elevation, flooding would have occurred for Scenarios S2 and S3 before any tsunami waves have arrived at the study area (Table 4). Low-lying areas of the Campbell River valley would be flooded. Low lying areas in Greater Vancouver will also require added protection for global sea level rise Scenarios 2 and 3.

- The tsunami at Boundary Bay will reach heights of up to 1.6 m above the tidal level at the time of the wave arrivals for all scenarios (Table 3). The first wave will be the highest. Corresponding wave heights at Semiahmoo will be up to 1.3 m. For all sites in Boundary Bay, tsunami wave amplitudes only weakly depend on the initial sea level applied to the model, and hence on the overall effect of global sea level rise.

- The distribution of modelled tsunami wave amplitudes in Boundary Bay is non-uniform, with highest waves occurring toward the end of the bay (Mud Bay) and in Drayton Harbor; the distribution of wave amplitudes along the Semiahmoo coast is nearly uniform. Differences in the distribution of tsunami waves heights among the three sea level rise scenarios are small.

- The tsunami will induce moderate currents at the entrance to Drayton Harbor (up to 4 m/s), at the mouth of the Nicomekl River (up to 3 m/s) and at the mouth of the Campbell River (up to 2 m/s). With sea level rise, current speeds increase at the mouths of the rivers, but decrease at the entrance to Drayton Harbor.

- At Site 8, immediately south of the Nicomekl River near Mud Bay, the wave-induced current is up to 1.35 m/s for all scenarios, while for other sites, the current does not exceed 1 m/s for all sea level rise scenarios.
- In the case of Scenario-3 (global sea level rise of 2.0 m), tsunami waves will overflow in some places even for the updated dike presented here, causing flooding along the Mud Bay coast and in Boundary Bay Park. These areas require additional protection.

Because details of future tsunamis remain unknown in many aspects, we recommend the use of a safety factor of 50%, which should be added to the tsunami amplitudes estimated for a magnitude M_w 9.0 CSZ event. The risk of flooding increases with increases in global sea level. Although the results of the tsunami modeling show that tsunami wave parameters are only weakly modified by the initial sea level, the arrival of tsunami waves during times of future elevated initial sea levels will markedly increase the maximum water heights at the time of the tsunami.

ACKNOWLEDGEMENTS

This project was funded through "Coastal Flood Mitigation Canada" within the Defence Research and Development Canada's Centre for Security Science (DRDC CSS) Program (CSSP), led on the Pacific Coast by Nicky Hastings of the Geological Survey of Canada, Natural Resources Canada. Her support, and that of our colleagues, throughout the program is gratefully acknowledged. We thank Tomas James (Natural Resources of Canada) for providing the digital sea level rise maps, Marlene Jeffries (Canadian Hydrographic Service) and Mark Rankin (Ocean Networks, Canada) for providing us with the high-resolution bathymetric and topographic data for the Boundary Bay region and for helping with the vertical datum adjustment. The authors gratefully thank Kelin Wang (Geological Survey of Canada, Natural Resources Canada) for providing us the latest source model for the CSZ earthquake and tsunami. Alexander Rabinovich helped reformat the original report for the Canadian Technical Report series. The final version was reviewed for publication by Neil Dangerfield of the Institute of Ocean Sciences (Fisheries and Oceans, Canada).

REFERENCES

AECOM (2013), *Modelling of Potential Tsunami Inundation Limits and Run-Up*, Capital Regional District, Project No. 6024 2933, 36 p.

Atwater, B.F., Nelson, A.R., Clague, J.J., Carver, G.A., Yamaguchi, D.K., Bobrowsky, P.T. et al. (1995), Summary of coastal geologic evidence for past great earthquakes at the Cascadia subduction zone. *Earth Spectra* 11(1):1–18

British Columbia 3-arc-second Bathymetric Digital Elevation Model (2017), https://www.ngdc.noaa.gov/metaview/page?xml=NOAA/NESDIS/NGDC/MGG/DEM/iso/xml/4956.xml&view=getDataView&header=none.

Cherniawsky, J.Y., Titov, V.V., Wang, K., and Li, J.-Y. (2007), Numerical simulations of tsunami waves and currents for southern Vancouver Island from a Cascadia megathrust earthquake, *Pure and Applied Geophysics*, 164 (2-3), 465-492, doi:10.1007/s00024-006-0169-0.

Cheung, K.F., Wei, Y., Yamazaki, Y., and Yim, S.C.S. (2011), Modeling of 500-year tsunamis for probabilistic design of coastal infrastructure in the Pacific Northwest, *Coastal Engineering*, 58 970–985

Clague, J.J., Bobrowsky, P.T., and Hutchinson, I. (2000), A review of geological records of large tsunamis at Vancouver Island, British Columbia, and implications for hazard, *Quaternary Science Reviews,* 19, 849-863.

Clague, J.J., Munro, A., and Murty, T.S. (2003), Tsunami hazard and risk in Canada, *Natural Hazards* 28 (2-3), 433-461.

Dragert, H., and Rogers, G.C. (1988), Could a megathrust earthquake strike southern British Columbia? *GEOS*, 17 (3), 5-8.

Fine, I.V., Cherniawsky, J.Y., Rabinovich, A.B. and Stephenson F.E. (2008), Numerical modeling and observations of tsunami waves in Alberni Inlet and Barkley Sound, British Columbia, *Pure and Applied Geophysics*, 165, (11/12), 2019-2044.

Fine, I.V., Thomson, R.E., Lupton, L.M., and Mundschutz, S. (2018), *Numerical Modelling of a Cascadia Subduction Zone Tsunami at the Canadian Coastal Base at Victoria, British Columbia*. Canadian Technical Report of Hydrography and Ocean Sciences, 324: v + 30p.

Fine, I., Thomson, R., and Hastings, N., 2023. Numerical simulation of a Cascadia Subduction Zone tsunami with application to Boundary Bay in the southern Strait of Georgia. Canadian Technical Report of Hydrography and Ocean Sciences, 368: v + 39 p.

Gao, D., Wang, K., Insua, T.L., Sypus, M., Riedel, M. and Sun Tiahaozhe, S. (2018), Defining megathrust tsunami source scenarios for northernmost Cascadia. *Natural Hazards*, 94**,** 445–469 (2018). https://doi.org/10.1007/s11069-018-3397-6

GEBCO One Minute Grid, The. Version 2.0 (2014), http://www.gebco.net.

National Tsunami Hazard Mapping Program (NTHMP) (2010), *Guidelines and Best Practices for Tsunami Inundation Modeling for Evacuation Planning*. NTHMP Mapping & Modeling Subcommittee, NOAA, USA.

Ng, M.K.-F., LeBlond, P.H., and Murty, T.S. (1990), Numerical simulation of tsunami amplitudes on the coast of British Columbia due to local earthquakes, *Science of Tsunami Hazards*, 8, 97-127.

Ng, M.K.-F., LeBlond, P.H., and Murty, T.S. (1991), Simulation of tsunamis from great earthquakes on the Cascadia subduction zone, *Science*, 250, 1248–1251.

Satake, K., Shimazaki, K., Tsuji, K., and Ueda, K. (1996), Time and size of a giant earthquake in Cascadia earthquake inferred from Japanese tsunami records of January 1700, *Nature*, 379, 246–249.

Stocker, T.F., Qin, D., Plattner, G.-K., Tignor, M., Allen, S.K., Boschung, J., Nauels, A., Xia, Y., Bex, V., and Midgley, P.M. (eds.), *Climate Change 2013: The Physical Science Basis. Contribution of Working Group I to the Fifth Assessment Report of the Intergovernmental Panel on Climate Change*, Cambridge University Press, Cambridge, United Kingdom and New York, NY, USA, 1535 pp.

Whitmore, P.M. (1993), Expected tsunami amplitudes and currents along the North American coast for Cascadia Subduction Zone earthquakes, *Natural Hazards*, 8, 59–73.